Genetic Analysis of the Quorum Sensing Regulator EsaR

Jessica M. Koziski

Thesis submitted to the faculty of the Virginia Polytechnic Institute and State University
in partial fulfillment of the requirements for the degree of

Master of Science
in
Biological Sciences

Ann M. Stevens, Chair
Timothy J. Larson
Zhaomin Yang

July 24, 2008
Blacksburg, VA 24061

Key words: quorum sensing, *Pantoea stewartii* subsp. *stewartii*, EsaR, repressor, mutagenesis, dimerization

Genetic Analysis of the Quorum Sensing Regulator EsaR

Jessica M. Koziski

Abstract

Pantoea stewartii subsp. *stewartii* is the causative agent of Stewart's wilt disease in maize plants. The bacteria are injected into the plant by corn flea beetles during feeding. They colonize the xylem and overproduce a capsular exopolysaccharide (EPS) at high cell densities. The production of EPS is regulated by an EsaI/EsaR quorum sensing mechanism, homologous to the LuxI/R system. Although activation of the EPS encoding genes by EsaR occurs after it complexes to the AHL (3-oxo-C6-HSL), unlike the LuxI/R system, this activation occurs by a different mechanism. At low cell densities, dimerized EsaR acts as a repressor. At a high cell population, derepression of the EPS genes occurs via an unknown mechanism once the AHL complexes to EsaR. Hence, a random mutagenesis genetic approach to isolate EsaR* variants that are immune to the effects of AHL has been utilized. Error-prone PCR and site-directed mutagenesis were used to generate desired mutants, which were subsequently screened for their ability to repress transcription in the presence of AHL. Several individual amino acids playing a critical role in the AHL-insensitive phenotype have been identified and mapped onto a homology model of EsaR. A separate study attempted to localize the dimerization region and analyze the stability of the N-terminal domain of EsaR. Truncations of EsaR at amino acids 169 and 178, without and with the extended linker region respectively, were generated using PCR. Dimerization assays similar to those by Choi and Greenberg in 1991 were performed but proved to be unsuccessful. However, the N-terminal domain is stable as determined by western blotting, which may facilitate its future structural

analysis. Together, these efforts have contributed to the molecular understanding of AHL-dependent derepression of EsaR.

Acknowledgements

I would like to thank Ann Stevens for always having time for me, offering support, guidance, and encouragement when I needed it. You've helped me to become a better graduate student and a better scientist in so many ways. Thank you for always having our best interests at heart.

To my committee members: Tim Larson and Zhaomin Yang, thank you for all of your suggestions, help, and perspectives on my thesis projects. It has undoubtedly made my work stronger.

I would like to thank Carla Finkelstein for teaching me how to use PyMOL, and for helping me to separate EsaR from TraR and LuxR in the .pdb file.

For help with the protein melting assay protocol and RT-PCR programming I would like to thank Cory Bernards. I thank Dr. Florian Schubot for the data analysis of this assay, and for answering my questions in protein chemistry.

I thank Robert White for his help with the fluorescence spectrometer, providing suggestions, and troubleshooting my experiment. I also would like to thank Laura Grochowski for all of your kindness in providing control samples for fluorescence spectroscopy and for your help with this experiment as well.

For sharing all of your protocols with me, answering my questions, giving me a different perspective on my results, and generating the plasmid for blue/white screening described in Chapter II, I am immensely grateful to Daniel Schu.

To the members of the Stevens Lab: Danny, Josh, Deric, and Nan, I am grateful for the fun and laughter the past two years. Thank you for your friendship and ability to make being in the lab never seem like work.

Last, but not least, I owe a huge debt of gratitude to my family and my fiancé Chris for their unyielding love and support. I cannot fathom how I would have completed the past two years without all of you by my side. To Chris, I am especially thankful. Thank you for all of your patience, optimism, and unconditional love.

This work was funded by a subcontract from NIH ROI GM066786.

Table of Contents

Table of Contents

List of Figures

List of Figures (cont.)

List of Tables

Chapter I

Literature Review

Quorum sensing is a cell-cell communication system found among a wide variety of bacteria. As its name suggests, bacteria are able to sense a dense population, or quorum, through a diffusible signaling molecule termed autoinducer (AI) (Fuqua and Greenberg, 2002; Reading and Sperandio, 2007). As the AI accumulates and reaches a critical threshold concentration it specifically binds to a regulatory protein, or in some bacteria activates a two-component regulatory system, which regulates gene expression by binding to target promoter sequences. The AI-protein-DNA complex allows for bacterial coordination of gene expression through the activation or repression of downstream genes, resulting in the regulation of production of virulence factors, secondary metabolites, biofilms, motility, and bioluminescence among other physiological processes (Joint et. al, 2007).

The connection between bioluminescence and quorum sensing in *Vibrio fischeri*

Bioluminescence, catalyzed by luciferase, has long been known to occur in a variety of marine organisms, both eukaryotic and prokaryotic (Wilson and Hastings, 1998; Visick and Ruby, 2006). A model for the dependence of this phenotype in relation to quorum sensing has been developed using the marine bacterium, *Vibrio fischeri*, a symbiont of the Hawaiian bobtail squid *Euprymna scalopes* (Smith et al, 2006). The bacteria are retained within the squid through a specialized organ named the light organ where they can grow up to a density of 10^{10} cells/ml (Boettcher and Ruby, 1990; Visick and McFall-Ngai, 2000). At this dense aggregation, bioluminescence occurs and is used to prevent the squid from casting a shadow in a phenomenon called counter-illumination, believed to help camouflage the squid from its predators (McFall-Ngai, 1990; Ruby, 1996; Fuqua and Greenberg, 2002). As morning approaches the squid flushes or vents

the bacteria from the light organ into the open seawater leaving approximately five to ten percent of the bacteria within the organ (Lee and Ruby, 1994). The remaining organisms then repopulate the squid's light organ over the course of the day so that bioluminescence will be available for counter-illumination during the evening (Visick and McFall-Ngai, 2000).

A formal connection between bioluminescence in squid and the quorum sensing phenomenon was established in 1970 by Nealson, Platt, and Hastings (Nealson et al, 1970; Fuqua and Greenberg, 2001). The activity of the luciferase enzyme was observed in *V. fischeri* as a function of cell growth. In a fresh inoculum it was found that the enzyme was not produced or the gene was inactive; however, during exponential phase luciferase levels rapidly rose in a short time span. Due to its presence later in the growth phase the authors concluded that the phenomenon occurred as a result of a "conditioning" of the medium by bacteria, the bacterial cells were producing an extracellular molecule as a result of their growth. This compound was later found to be the AI, its name derived from the word Nealson et al coined, autoinduction (Nealson et al, 1970).

Gene organization and function of the *lux* operon

A further understanding into the molecular mechanism of quorum sensing in *V. fischeri* has been the culmination of decades of research. It is representative of a typical quorum sensing system in Gram-negative proteobacteria (Bassler, 2002). This molecular characterization began after the isolation of a 9 Kb DNA fragment containing all elements believed necessary for bioluminescence (Engebrecht et al, 1983). By mutagenizing the fragment with transposon insertions, seven genes, called *lux* genes, were identified and found to be organized in two, divergent, transcriptional units

(Engebrecht and Silverman, 1984 and 1987). One unit contains solely the *luxR* gene, while the other is arranged in what is called the *lux* operon as *luxICDABE* (Figure 1.1). Subsequently, genes involved in the regulation of bioluminescence and in the activation of the *lux* operon have been identified in multiple bacterial species (reviewed in Smith et al, 2006). An additional gene, now included in the organization of the *lux* operon in current literature, is downstream of *luxE* and termed *luxG* (Swartzman et al, 1990; Nijvipakul et al, 2008).

Encoded within the operon is the heterodimeric enzyme, luciferase. Luciferase is comprised of an α and a β subunit, encoded by *luxAB* respectively (Meighen, 1991). Oxygen from the surrounding environment is used by luciferase to catalyze the oxidation of a long chain fatty aldehyde and a reduced riboflavin phosphate (Meighen, 1991; Bassler, 1999). During this reaction, an unstable intermediate emits a photon of blue-green light. The long chain aldehyde substrate is contributed to the reaction by LuxCDE, the translational products of *luxCDE*, which comprise a fatty acid reductase complex. The $FMNH_2$ substrate is donated to luciferase by LuxG, which has recently been shown to function as a flavin reductase (Nijvipakul et al, 2008). The activation of the *lux* operon is controlled by the transcriptional regulator, LuxR, and its cognate AI synthesized by LuxI (Eberhard *et al*., 1981; Whitehead *et al* 2001).

Acyl-homoserine lactone formation and structural diversity

The AI molecule produced by LuxI was the first acyl-homoserine lactone (AHL) to have its structure elucidated through the use of ^{1}H nuclear magnetic resonance spectroscopy, infrared spectroscopy, as well as high-resolution spectrometry (Eberhard et al, 1981; Fuqua and Greenberg, 2002). Formally called N-3-oxo-hexanoyl-L-homoserine

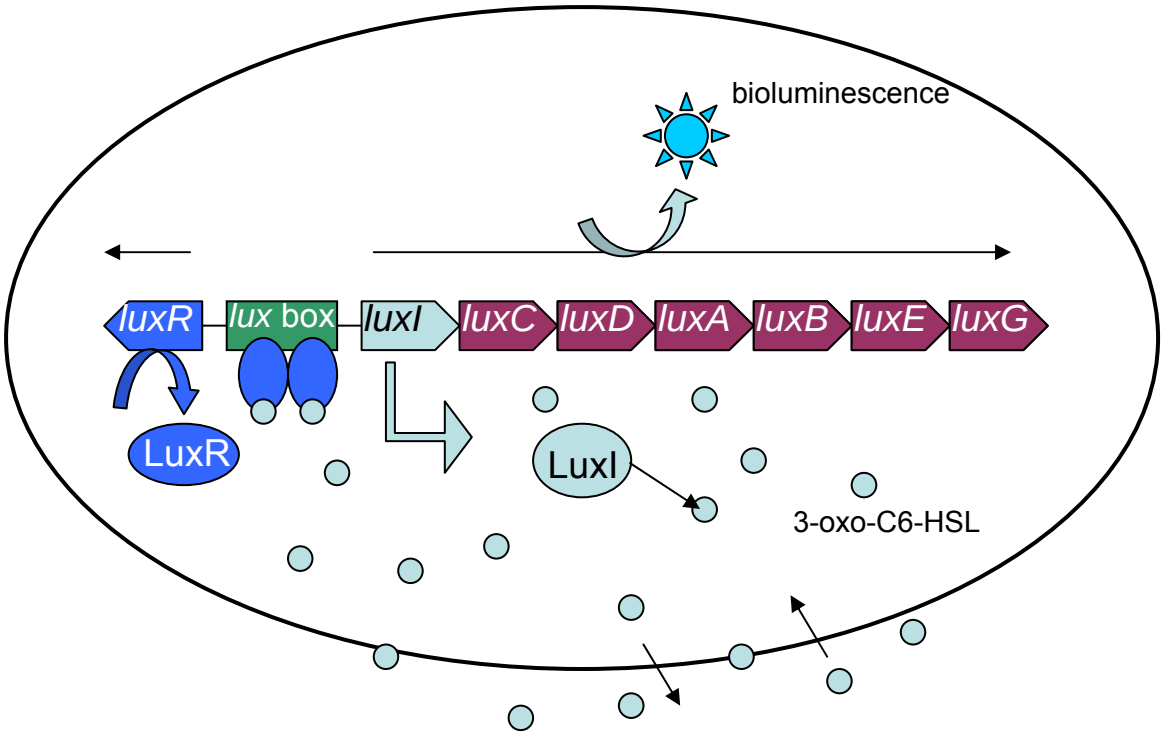

Figure 1.1. Model of the quorum sensing mechanism of *V. fischeri* at high population densities Once the population density reaches a high density, the autoinducer (small circles) produced by LuxI forms complexes with the regulatory protein LuxR to form a homodimer, which binds to the *lux* box and activates transcription of the *lux* operon. The result is bioluminescence output.

lactone, it consists of a 6 carbon fatty acyl chain linked to the lactonized homoserine ring via an amide bond. It is synthesized from two compounds, S-adenosyl-L-methionine (SAM) and an acylated acyl carrier protein (acyl-ACP) (More et al, 1996; Schaefer et al, 1996). The AHL synthase, and homologous proteins, form the AHL by first binding to SAM followed by its interaction with the acyl carrier protein. LuxI then subsequently catalyzes the transfer of the acyl group from the acyl-ACP to the amine of SAM (Pappas et al, 2004).

Since the initial finding of AHL, a multitude of Gram-negative proteobacterial species that produce acyl-HSL have been identified, however, there is structural variation of the acyl chain among the species. This is believed to provide specificity of LuxR and its homologues to its cognate AHL (Nasser and Reverchon, 2007). The length may vary in the number of carbon atoms, containing anywhere from four to eighteen atoms commonly found in increments of two (Watson et al, 2002; Pappas et al, 2004). Enhancing the acyl-HSL diversity among the bacterial species is the chemical state of the third carbon in the acyl chain, whose oxidation/reduction state is dependent upon the presence or absence of a substituted hydroxyl group or keto group.

AHL synthases

A bioinformatics study of 35 AHL synthase proteins found that despite their homologous function and 27-53% sequence identity, the predicted and solved structures of the proteins are divergent (Chakrabarti and Sowdhamini, 2003; Gould et al, 2004). This divergence is best illustrated by the acyl-ACP binding pocket of crystallized EsaI of *Pantoea stewartii* subsp. *Stewartii* and LasI of *Pseudomonas aeruginose*, proteins that synthesize 3-oxo-C6-homoserine lactone and 3-oxo-C12-homoserine lactone respectively

(Nasser and Reverchon, 2007). Within LasI, the binding pocket consists of an open tunnel conformation in which the twelve carbon acyl chain can bind, providing LasI the ability to catalyze long-chained acyl-HSL. In contrast, the acyl-ACP binding pocket of EsaI is more confined, only neatly allowing the six carbon atom acyl chain to interact with EsaI (Watson et al, 2002). Additional AHL synthase deviation can be observed in the interaction of acyl-ACP to LasI or EsaI resulting in slight structural changes of the synthase (Watson et al, 2002).

The longer acyl chain used by LasI of *Pseudomonas aeruginosa* allows for its higher binding affinity to the "tunnel", permitting a low binding energy of the ACP-LasI interaction (Gould et al, 2004). In contrast short-chained acyl-ACP in EsaI of *Pantoea stewartii* subsp. *stewartii* must counteract a higher binding energy relative to the long acyl-ACP, by inducing a greater interaction between the synthase and ACP. Unlike LasI, this induces a conformational change in EsaI and subsequently allows the open N-terminal position of SAM to be in a catalytically allowable configuration. Contrarily, the low binding energy of LasI to ACP as well as having a closed, catalytically competent N-terminal arrangement reduces the need for conformational changes in the enzyme.

Mechanistic involvement of AHL with transcription factors

Due to both the hydrophobic nature of the acyl chain and the hydrophilic homoserine lactone ring, the AHL molecule is amphipathic. This allows most AHLs to pass through the cell's phospholipid bilayer and traverse through the intracellular fluid to form a complex with LuxR and other LuxR-type proteins under high cell density conditions; or in a confined area with restricted AI diffusion (Fuqua et al, 2001; Waters and Bassler, 2005; Gonzalez and Keshevan, 2006). The LuxR-type-protein-AI

interaction takes place on the N-terminal domain (NTD), which is one of the two binding domains of the regulatory protein. The C-terminal domain (CTD) is involved in DNA binding (Choi and Greenberg, 1991; Choi and Greenberg, 1992; Stevens and Greenberg, 1997).

In response to the AHL-NTD interaction, LuxR is activated and forms a homodimer, which is capable of binding to the DNA. The DNA binding site is termed the *lux* box and is positioned -42.5 base pairs upstream from the transcriptional start site of the *lux* operon (Stevens and Greenberg, 1997; Stevens and Greenberg, 1999). The DNA sequence is twenty base pairs long and contains dyad symmetry, or is palindromic, and offers a binding site to AHL-LuxR recognized by the helix-turn-helix motif located at the C-terminal end of LuxR. Genetic and biochemical studies have shown that AHL-LuxR binds to the *lux* box and subsequently contacts the RNA polymerase at the alpha-CTD and sigma subunit, reminiscent of class II type promoters (Devine, et al, 1989; Stevens and Greenberg, 1997; Finney et al, 2002; Johnson et al, 2003). Once the AHL-LuxR binds to the *lux* box and interacts appropriately with the RNAP, transcription of the *lux* operon and bioluminescence occurs.

Gram-positive quorum sensing

Since Nealson, Platt, and Hastings' initial work in *V. fischeri*, quorum sensing systems have been found in more than 50 Gram-negative proteobacteria (Fuqua et al, 2001). Moreover, quorum sensing is not limited to Gram-negative bacteria, but has since been identified in Gram-positive bacteria as well.

The signaling system in Gram-positive bacteria is vastly different from that of Gram-negative bacteria. The AI in this classification originates as a precursor

oligopeptide, which undergoes modifications by the cell to become biologically active (Taga and Bassler, 2003). Since the oligopeptide is not readily diffusible across the cell membrane, the autoinducer is recognized extracellularly by specific transmembrane proteins (Waters and Bassler, 2005). Like Gram-negative bacteria, at high cell densities, the signal reaches a critical threshold where the oligopeptide can interact with a membrane-bound histidine kinase sensor protein (Reading and Sperandio, 2006). This protein then interacts with a cytoplasmic response regulator protein, and activation of target gene expression occurs through a phosphoryl-relay system (Figure 1.2). A well-characterized quorum sensing system in Gram-positive bacteria is the opportunistic pathogen, *Staphylococcus aureus*, which responds to an extracellular peptide concentration to produce biofilms (Kong et al, 2006). Other Gram-positive, quorum sensing organisms include *Streptococcus faecalis* and *Streptococcus pneumoniae* (Cvitkovitch et al, 2003).

Quorum sensing by AI-2

An additional signaling molecule found in Gram-positive bacteria as well as Gram-negative bacteria is the widely conserved, universal AI, AI-2, produced by LuxS (Lyon and Novick, 2004; Gonzalez and Keshavan, 2006; Keersmaecker et al, 2006). Initially detected by Bassler et al in 1994 in the marine bacterium, *Vibrio harveyi*, the AI is unique in its structure, a furanosyl borate diester, and is produced from SAM in three enzymatic steps (Chen et al, 2002). The conservation of LuxS has also been attributed to its alternative function in the cell as a catalyst in the activated methyl cycle, which provides methyl groups for DNA and proteins (Vendeville et al, 2005). A result of this catalysis is AI-2.

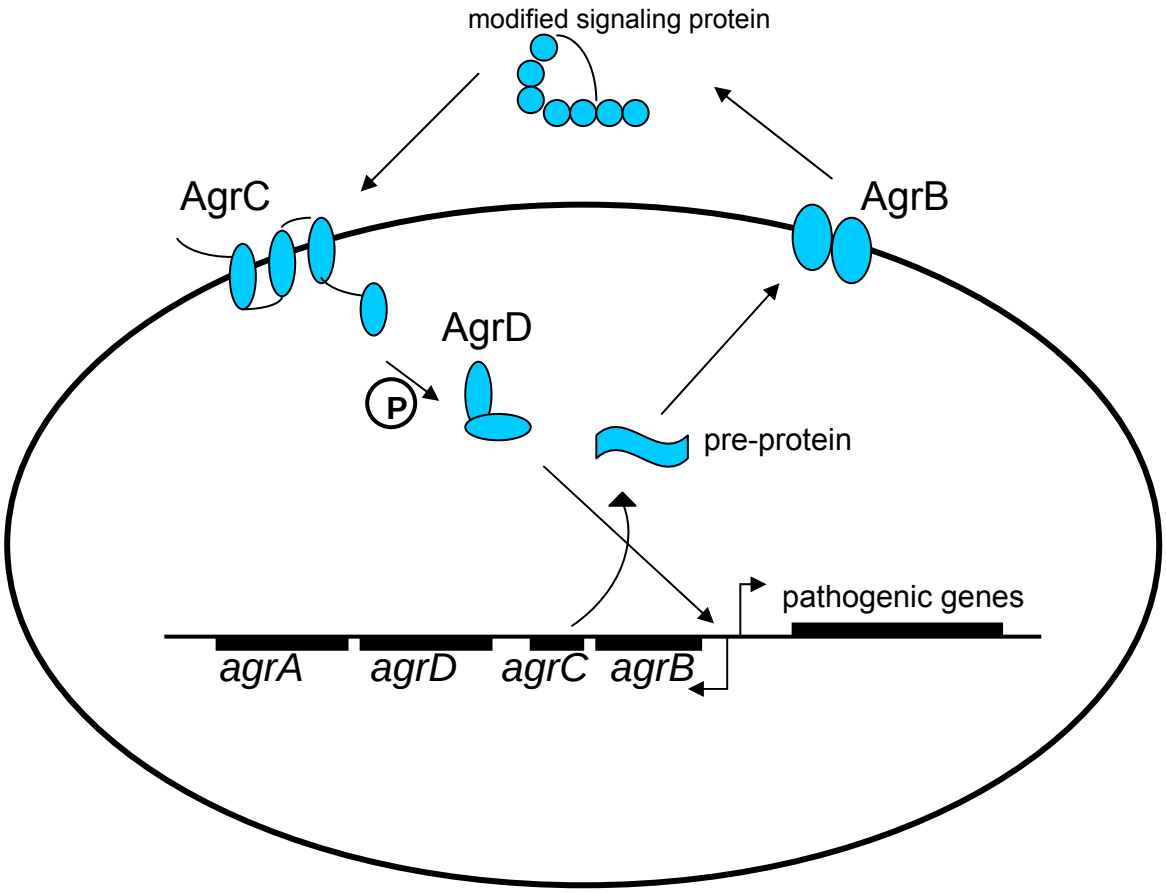

Figure 1.2. Model of the quorum sensing mechanism in *S. aureus*. In a high cell population density, the *agr* operon produces a peptide signal from *agrD* (pre-protein) which is both modified to approximately 8 amino acids and subsequently transferred to the extracellular medium by AgrB. At a critical threshold the peptide binds to AgrC, a hisitidine-kinase, to activate the response regulator AgrD. AgrD then activates a positive feedback loop as well as the genes involved in biofilm production.

Despite the dual roles of LuxS, its role in quorum sensing is strongly supported by numerous publications in recent years, especially in relation to its use by the model organism, *V. harveyi* (Vendeville et al, 2005). In *V. harveyi*, the absence of AI-2 leads to the phosphorylation of LuxO via LuxU whereby it interacts with sigma factor 54 to activate the transcription of regulatory small RNAs (sRNA) (Defoirdt, et al, 2008). The sRNAs form a complex with the chaperone protein, Hfq, and are then able to interact with the mRNA of $LuxR_{VH}$. $LuxR_{VH}$ is an activator of the *lux* operon. The mRNA-Hfq-sRNA interaction causes destabilization of the mRNA, leading to the absence of the $LuxR_{VH}$ protein and reduced bioluminescence (Vendeville et al, 2005). In contrast, at a high cell concentration, the AI-2 acts in concert with two other signaling molecules. One (AI-1) binds to LuxN while the second (AI-2) binds to a periplasmic binding protein, LuxP, which causes a conformational change in a membrane protein LuxQ (Neiditch et al, 2005). The third autoinducer (CAI-1) is produced by CqsA and is recognized by CqsS (Defoirdt et al, 2008). The binding of the autoinducers to their respective receptor proteins causes these membrane proteins to exhibit phosphatase activity, leading to the dephosphorylation of LuxO by LuxU. The inactivated LuxO cannot produce the sRNAs and thus bioluminescence occurs (Waters and Bassler, 2005) (Figure 1.3). Other examples of AI-2 regulated quorum sensing are involved in pathogenesis. This includes the regulation of the cholera toxin and the co-regulated pili in *Vibrio cholerae*, as well as the regulation of VirB in *Shigella flexneri* (Reading and Sperandio, 2007). **Inter-kingdom quorum sensing**

LuxS and its cognate autoinducer, AI-2, was initially believed to regulate the production of the type III secretion and motility in *E. coli* O157:H7 as well (Sperandio et

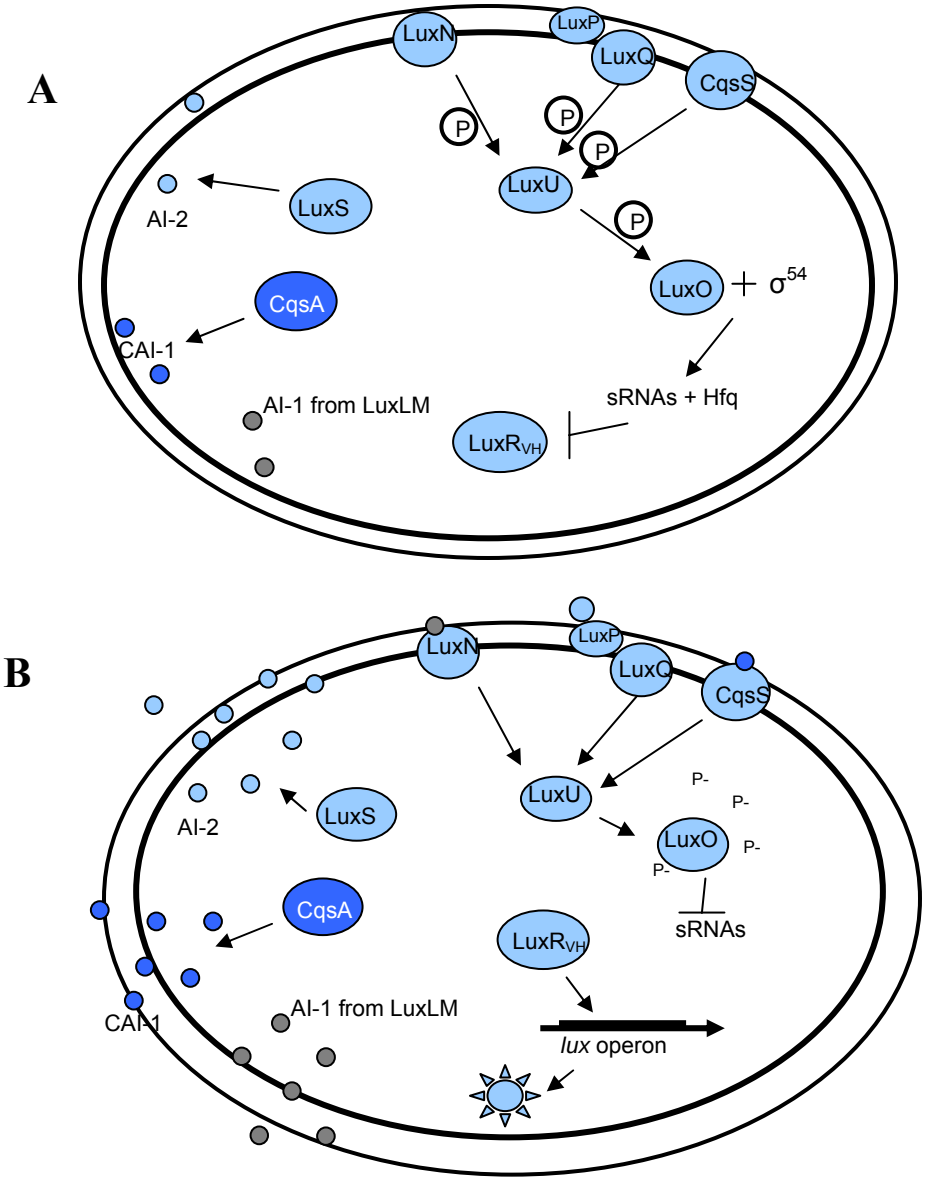

Figure 1.3. A simplified illustration of quorum sensing in *V. harveyi* by AI-2. *V. harveyi* produces three AI molecules, AI-1, AI-2, and CAI-1 produced by LuxLM, LuxS, and CqsA respectively. AI-1 is recognized by the membrane protein LuxN, AI-2 binds to the periplasmic binding protein, LuxP, while CAI-1 binds to the membrane protein CqsS. **A.** In the absence of all AIs, the receptor proteins phosphorylate LuxU, which in turn phosphorylates LuxO. This activated protein in conjunction with a sigma factor is then capable of transcribing small regulatory RNAs which forms a complex with the molecular chaperone Hfq, causing the mRNA of $LuxR_{VH}$ to be unstable. **B.** When a high concentration of AIs is present and bound to their respective protein, the receptor proteins switch from kinases to phosphatases causing LuxU to dephosphorylate LuxO. LuxO does not activate the production of the sRNAs and $LuxR_{VH}$ is produced, allowing for bioluminescence.

al, 1999; Sperandio et al, 2001). Strains that lacked a functional *luxS* were unable to activate the operon for type III secretion and motility, and complementation of the *luxS* gene in *trans* re-established the activation of these operons. However, when purified AI-2 was added exogenously to strains with a knocked out *luxS* gene, the wild-type phenotype was unable to be restored (Sperandio et al, 2003). This led to the identification of a new LuxS-dependent autoinducer (termed AI-3) that is responsible for the activation of pathogenic genes termed AI-3 (Walters et al, 2006).

AI-3 has since been found to not be the sole factor involved in activating the pathogenic *E. coli* operons, but rather acts synergistically with the host signaling molecules, epinephrine and norepinephrine (Sperandio et al, 2003). Current opinion is that as the bacteria come into close proximity with the host epithelial cells, the hormones alter bacterial gene expression, one consequence of which is the allowance of cell attachment through the expression of motility genes. The altered expression also allows for further activation of virulence genes by AI-3 (Kendall et al, 2007). The EHEC strain is able to sense the eukaryotic hormones as well as AI-3 through the membrane protein, QseC (Kendall et al, 2007). QseC, a sensor kinase, is part of a two-component regulatory system that activates the response regulator QseB in response to the binding of AI-3/epinephrine/norepinephrine. QseB, in turn, activates pathogenic EHEC genes (Figure 1.4). While the structure of AI-3 is unidentified, it is believed to be similar in structure to epinephrine/norepinephrine due to the ability of QseC to recognize the bacterial and host signals (Sperandio et al, 2003).

The LuxR protein family

As has been described above, while the phenomenon of quorum sensing has been

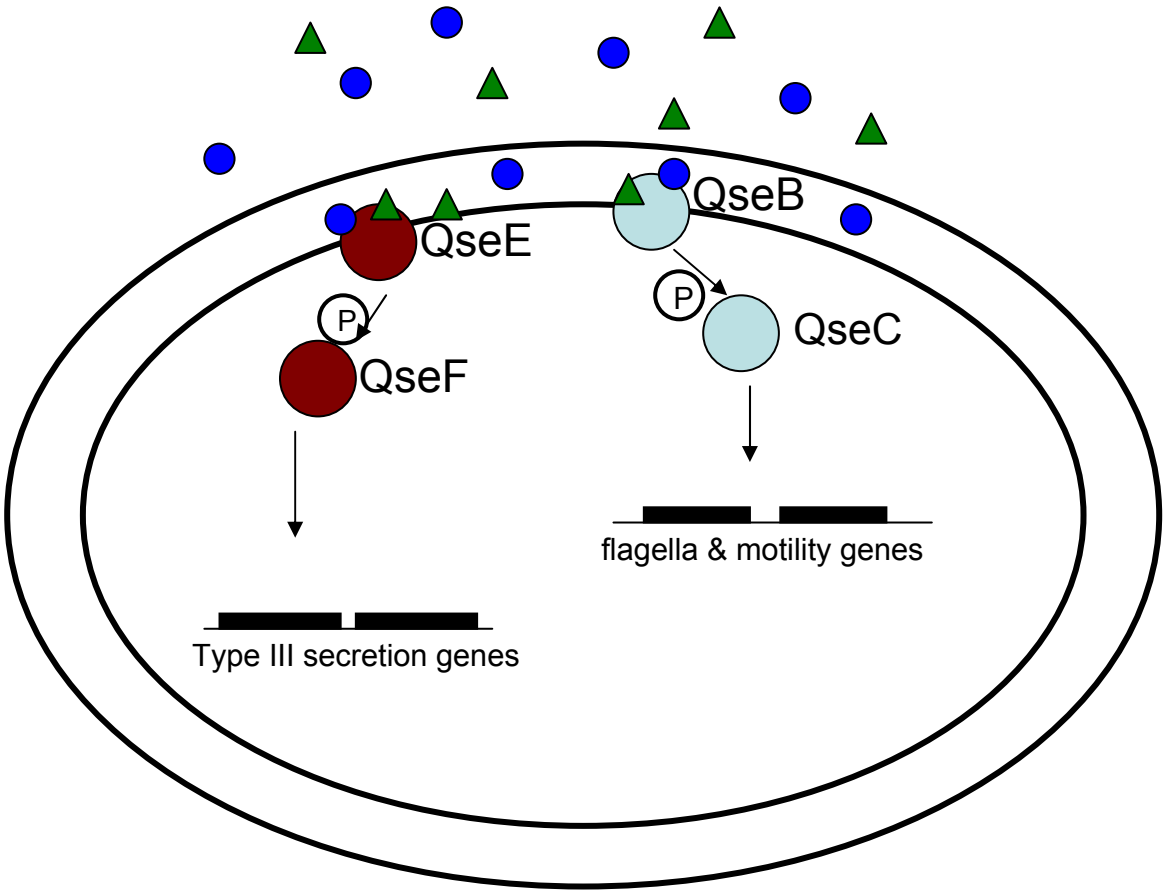

Figure 1.4. Current quorum sensing model in enterohemorrhagic *E. coli* by AI-3. Both AI-3 (small circles) and epinephrine/norepinephrine (triangles) are capable of binding to and activating the two-component regulatory system QseBC. Once phosphorylated, QseB in turn activates the expression of genes required for motility. The same signaling molecules are thought to bind to a second two-component regulatory system, QseEF, to activate type-III secretion genes.

conserved, the mechanism by which it occurs has not. Even on a smaller scale, diversity in quorum sensing has been found among Gram-negative proteobacteria. Further research into the molecular mechanisms of the over fifty LuxI/R-type systems has yielded structural and functional divergence within the homologous LuxR proteins. The diversity of such proteins has led to the proposition of a class organization based on its reliance on AHL for proper protein function as well as the mode of action of the AHL-LuxR-type complex (Greenberg, personal communication). The first class of proteins exhibits the ability of the AHL to reversibly bind to LuxR and its homologues and activate the transcription of downstream genes. One example already discussed in great detail is LuxR itself. The AHL appears to bind reversibly to LuxR whereby the complex makes contact with RNAP upon binding to the DNA, resulting in transcription of the *lux* operon and bioluminescence (Urbanowski et al, 2004).

A second class of activators relies on AHL as a scaffold for proper folding, resulting in an irreversible AHL-protein interaction. Evidence for this class proposal is based on the crystallization of a LuxR-type protein, TraR, found within the plant pathogen, *Agrobacterium tumefaciens*. *A. tumefaciens* uses the homologous quorum sensing proteins TraI/R to control the transfer of a conjugated Ti plasmid between bacteria, resulting in dissemination of the plasmid (Miller and Bassler, 2001). Like LuxI, TraI directs the synthesis of an AHL (3-oxo-C8-homoserine lactone). This AHL complexes with partially unfolded, disordered TraR at the N-terminal region, separated from the C-terminal region by a twelve base pair linker. Upon proper folding the AHL-TraR complex can then bind to regions of DNA called *tra* boxes, which are comprised of eighteen base pairs with dyad symmetry (White and Winans, 2007). Various genes

activated by the stable, asymmetric TraR homodimer include those for plasmid transfer and cell proliferation (Swiderska et al, 2001; Zhang et al, 2002).

Direct evidence for the requirement of AHL for proper TraR folding was provided after it was crystallized and the solved structure was achieved independently by two laboratories (Vannini et al, 2002; Zhang et al, 2002). Both studies reported that the signaling molecule is fully imbedded within the N-terminal region of the protein, surrounded by hydrophobic and aromatic residues. This suggests that the AHL may be instrumental for achieving the proper conformation of TraR as it is unlikely for the molecule to insert into post-folded TraR. Additionally, the interaction of the AI with conserved residues of TraR allows a dimerization region to be exposed among four alpha helices in the C-terminal domain, in addition to dimerization residues exposed within the N-terminal region, as a result of conformational changes. Once in the active state and bound to the DNA, it may contact the RNAP through conserved residues for the activation of transcription (Pappas et al, 2004; Zhang et al, 2002; Vannini et al, 2002).

Like TraR, the recent crystallization of the LuxR-type protein LasR provides further support for the second class of LuxR homologues (Greenberg, Personal Communication, Bottomley et al, 2007). LasR is one of many quorum sensing regulators in *P. aeruginosa* that helps to regulate the transcription of hundreds of genes (Schuster and Greenberg, 2006). *P. aeruginosa* is considered an opportunistic pathogen, infecting and often causing the death of immunocompromised patients by pneumonia, urinary tract infections, bloodstream infections, and biofilm production (Bottomley et al, 2007). Like the LuxI/R quorum sensing system, LasI constitutively produces the AHL molecule 3-oxo-C12-homoserine lactone. This AHL forms a complex with LasR at high cell

densities to activate the expression of virulence factors, in addition to regulating a second quorum sensing system called RhlI/R (Nouwens et al, 2003).

The crystal structure of LasR revealed that like TraR, LasR requires the AHL as a scaffold for appropriate folding and proper structural conformation (Bottomley et al, 2007). The stabilization of AI-LasR occurs via van der Waals interactions and hydrogen bonding within the hydrophobic core of LasR. The deeply imbedded AI also allows for the dimerization interface of the protein to be exposed upon correct folding of LasR due to structural changes upon binding. The 12-C acyl chain of LasR causes different structural changes once bound to LasR not seen within the AHL-TraR interaction. This results in differences in the orientation of the dimerization helices, allowing them to become more flexible, permitting LasR to be less restrictive in its binding to the promoter sequences. This may provide an explanation for the versatile regulatory nature of LasR. For example, while TraR requires dyad symmetry for DNA binding, LasR is able to bind both palindromic and non-palindromic sequences.

The third class of LuxR-type proteins serves as repressors

While research regarding the two classes of activators has been quite extensive, studies of the third class of LuxR-type proteins which negatively regulates quorum sensing systems, in the absence of AI, have been minimal (Nasser and Reverchon, 2007). In this system, the LuxR-type protein binds to and represses the transcription of downstream genes. Only in the presence of AI does derepression occur through a currently undefined mechanism. Proteins that fall under this classification include, but are not limited to, the LuxR homologues EsaR, ExpR, and EanR; all found within different plant pathogenic bacteria, and YenR from the human pathogen *Yersinia*

enterocolita (von Bodman et al, 2003; Castang et al, 2006; Morohoshi et al, 2007; Atkinson et al, 2006). Of these relatively few negative quorum sensing regulators identified, EsaR of *P. stewartii is* the best characterized and serves as a model of the LuxR-type repressors (Nasser and Reverchon, 2007).

Structurally, EsaR, as well as other known quorum-sensing repressors, contain differences within their amino acid sequence in comparison to other regulators of quorum sensing (Stevens, 1999). Like LuxR-type activators, the N-terminal region binds to the AHL and the C-terminal end binds to DNA. However, the repressors differ in that they contain an extended linker region between the two domains. Additionally, the C-terminal region is extended by several extra residues. These structural differences can be exemplified by a homology of EsaR, based on TraR, provided by M. Churchill (Figure 1.5).

The quorum sensing system of *P. stewartii* subsp. *stewartii*

P. stewartii produces a biofilm or capsular polysaccharide (CPS) which causes Stewart's wilt disease in maize plants (von Bodman and Farrand, 1995). In Stewart's wilt disease, the bacteria are transmitted into the plant by the corn flea beetle, *Chaetocnema pulicaria*, as they feed on maize seedlings (Pataky, 2003). *P. stewartii* is directly deposited into the plant tissue, where it migrates into the xylem and multiplies to a high density. This results in the production of the quorum sensing regulated CPS, and impedes the plant's normal vascular transport, causing wilt and necrotic lesions (Nimtz et al, 1996).

The genes involved in biofilm production in *P. stewartii* are indirectly regulated by an EsaI/EsaR quorum sensing mechanism which shares homology to the LuxI/R type

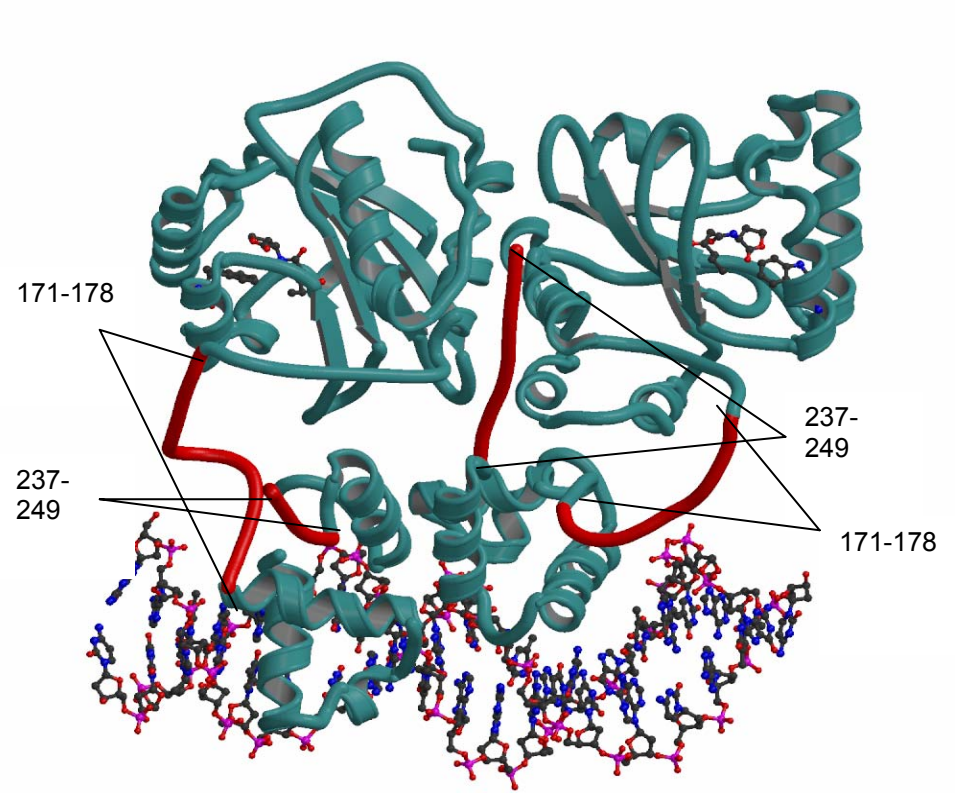

Figure 1.5. EsaR homology model based on the autoinducer associated TraR dimer-DNA structure (Zhang et al, 2002) kindly provided by A. Thode, D. Donham and M. Churchill. Cyan colored regions were generated from a threaded model. Red colored regions are repressor specific, residues 170-178 are located in the extended interdomain linker region and residues 241-249 consist of the extended C-terminus of EsaR, as labeled above. Both the AHL and DNA are shown as ball and stick.

system. EsaI is the AI synthase which produces the 3-oxo-C6-HSL that subsequently interacts with the transcription factor EsaR (von Bodman and Farrand, 1995). Although activation of the *cps* gene system occurs after EsaR complexes to the acyl-HSL, the stimulation is due to a derepression mechanism. Specifically, *P. stewartii* responds to a currently undefined external stimulus by the membrane protein RscF (von Bodman et al, 2008). RcsF then causes a phosphorelay system leading to the phosphorylation of RcsB, which interacts with RcsA. In low cell densities, where basal or low levels of acyl-HSL are being produced, EsaR was initially found to function as a repressor by binding to the promoter sequence and preventing the transcription of *rcsA*. Derepression of *rcsA* takes place when a threshold level of AI binds to EsaR at high cell population densities that in some way prevents EsaR from interacting with the DNA (Kouotsoudis *et al*, 2006). RcsA is then able to form a complex with the phosphorylated RcsB, which in turn binds to and activates the transcription of genes involved in the production of CPS (Figure 1.6).

Genetic evidence for the repression mechanism of EsaR and the *esaI*/*R* gene organization was shown through a mutational analysis of *esaI* and *esaR* by von Bodman et al in 1995 and 1998. Strains of *P. stewartii*, which were Δ*esaR* or Δ*esaIR*, constitutively expressed the CPS regardless of the cell density due to the lacking regulatory mechanism. Likewise, strains containing an *esaI* gene knockout were found to strictly repress the production of CPS irregardless of the cell concentration. Further confirmation of these observations occurred when the *esaR* promoter containing the EsaR binding site was fused to the *lacZ* gene and introduced into a strain containing the wild-type *esaR* in *trans*. The expression of *lacZ* dropped dramatically in comparison to a

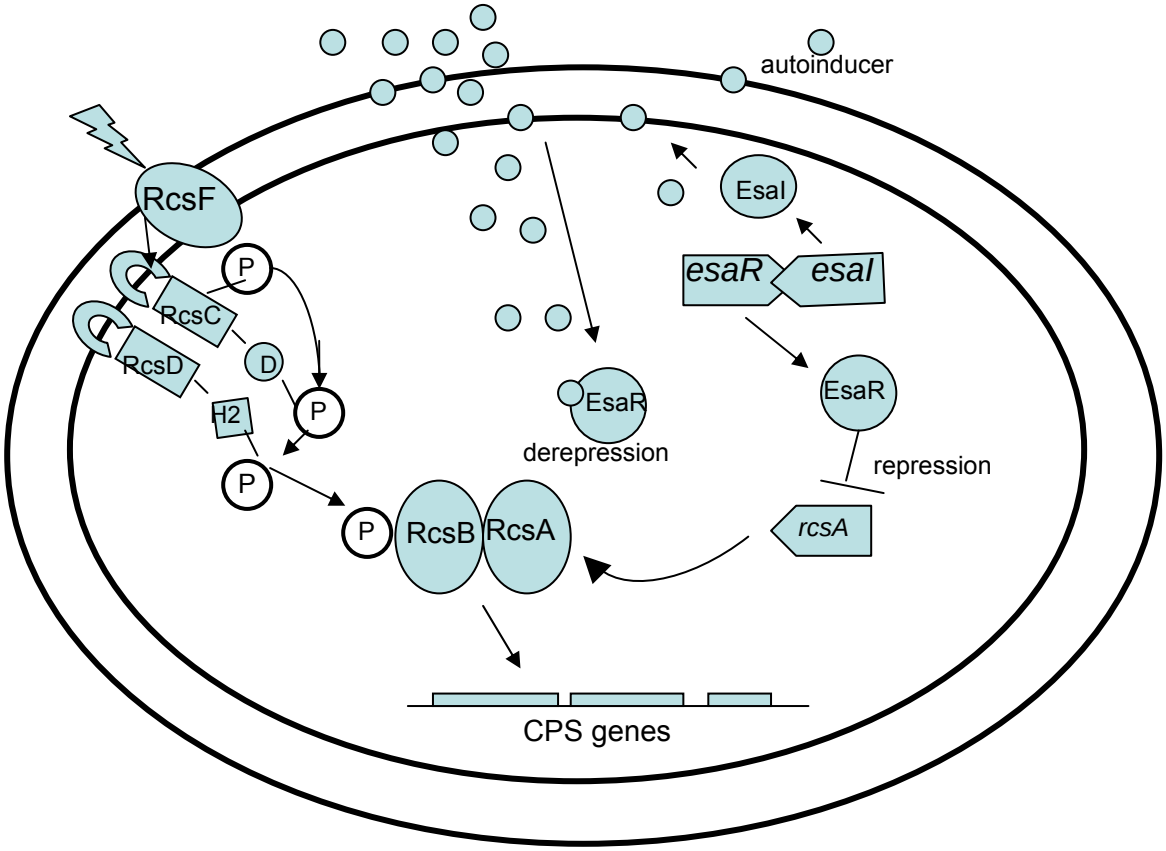

Figure 1.6. A model of repression by the LuxR-type protein, EsaR, in *Pantoea stewartii* subsp. *stewartii*. *P. stewartii* responds to an external stimuli, which stimulates a phospho-relay system ending with the phosphorylation of RcsB. In a low population density, EsaR represses *rcsA* expression. However, in a high cell density, the autoinducer, produced by EsaI, binds to EsaR and allows for derepression of *rcsA*. RcsA can then complex with phosphorylated RcsB and activate the transcription of the CPS genes.

strain which lacked functional EsaR. Moreover, a lack of involvement of EsaR in the regulation of the expression of *esaI* was observed through the creation of an *esaI*::*lacZ* fusion and introduction of *esaR* in *trans*. No effect was observed on AHL production or *lacZ* activity. These observations, coupled with sequencing, provide a clear picture of how the EsaI/R genes are organized within the chromosome. Proximately linked, *esaI* and *esaR* are convergently transcribed, sharing a sequence overlap of 31 base pairs. Detailed molecular analysis and infection studies of maize have since confirmed these conclusions as well (Minogue et al, 2002; Koutsoudis et al, 2006).

EsaR structure and function

Once folded in the correct conformation, EsaR binds to its target in the promoter region, termed an *esa* box, as a homodimer. The *esa* box is palindromic and overlaps the -10 box of the *esaR* promoter (Minogue *et al*, 2002). The sequence placement within the promoter is such that when EsaR binds to it, it blocks RNA polymerase from binding to the DNA and thus prevents transcription. This box is quite similar in nucleotide sequence to that of the *lux* box, differing in only five base pairs out of twenty. Due to the high degree of homology between the *lux* box and the *esa* box, EsaR is capable of binding to the *lux* box and activating the transcription of genes located downstream, though gene expression occurred to a lesser degree than with LuxR (von Bodman *et al* 2003). The study by von Bodman et al, 2003, further shows that the EsaR protein in the absence of AHL does retain its ability to bind to the *lux* box and interact with RNAP to activate transcription. In addition to its activation in the absence of AHL, de-activation of the *lux* operon occurred in its presence. These observations demonstrate the need for

a more detail structural analysis of the repressor class of LuxR homologues in order to fully comprehend their functions and divergence.

Research Plan

Despite the novelty of a quorum sensing regulator that acts as a repressor rather than an activator, research in elucidating the structural elements of EsaR in its interactions with AHL and DNA have been lacking in comparison to its activator homologues LuxR, TraR, and LasR (Nasser and Reverchon, 2007). Due to the insolubility of purified EsaR and its inability to crystallize, a deeper understanding of its mechanism of regulation must be carried out through genetic and biochemical testing. In this thesis project, genetic studies were performed to elucidate key amino acid residues involved in the AI-EsaR interaction through the random generation of EsaR* variants by error-prone PCR. These variants are capable of binding to DNA and repressing transcription of the downstream genes despite the presence of AHL, and have been identified through screening, and more quantitatively via β-galactosidase assays. Multiple mutations identified by sequencing, were dissected apart using site-directed mutagenesis. Subsequently, these EsaR* variants are being purified through the use of protein tags, and the affinity of EsaR* for the AHL will be determined by a variety of techniques, including a variation of differential scanning fluorimetry and fluorescence spectroscopy (Niesen et al, 2007; Minogue et al, 2002).

In addition to identifying the key amino acid residues in the AHL-EsaR interaction, a second project has been started, which will help to define the dimerization region of EsaR. Truncations of the protein were made within the extended linker region, where dimerization was hypothesized to occur, and subsequently transformed into an

Escherichia coli strain which contained the wild-type EsaR protein as well as the reporter gene, *lacZ*, each on different plasmids. Dominance assays then determined whether the truncations retained the dimerization region as they competed to form a dimer with the wild type. Ultimately, these mutagenesis studies of EsaR will provide a broader understanding not only of the EsaR subfamily, but will give insights into how AHL binding modulates the activity of quorum sensing transcriptional regulators.

Chapter II

Identifying Amino Acid Residues Involved in EsaR-AHL Interactions Through Random and Site-Directed Mutagenesis

Introduction:

To determine which specific amino acid residues are important for the EsaR-AHL interactions, *esaR* was randomly mutagenized through error-prone PCR. Interactions of interest include AHL binding by EsaR as well as its response to the ligand in overall conformation and DNA binding capacity. Following the random mutagenesis, AHL-independent variants were selected that constitutively repressed a *lacZ* fusion, controlled by the *esa* box located at -10 upstream of *lacZ*, in either the presence or absence of AHL. This repression assay relays two pieces of information. First, it indicates whether EsaR* is capable of binding to the *esa* box causing repression of *lacZ*. Second, if repression occurs despite the presence of AHL, then it is apparent that functional EsaR* is being produced within the cell. Colonies expressing the desired EsaR* variants differentially exhibited the desired white phenotype on 5-bromo-4-chloro-3-indolyl- beta-D-galactopyranoside (X-gal) plates. The activity of the EsaR* variants was subsequently verified through quantitative β-galactosidase assays and the genes encoding them were sequenced. The sites of mutation in variants which contained multiple substitutions were dissected apart using site-directed mutagenesis. The EsaR* variants with single substitutions were analyzed once again via repression assays, and their stability was examined by western immunoblotting. These efforts have identified 8 amino acids (AA) critical in the AHL-EsaR interaction.

Two additional methods were tested as the means to examine the AHL-binding capacity of the EsaR* variants: the protein melting assay and fluorescence spectrometry. The protein melting assay utilizes the increased thermal stability of EsaR in the presence of AHL (Minogue et al, 2002). Subsequent comparisons of thermal stability between

EsaR and EsaR* theoretically can indicate how crucial a role the residue plays in the AHL-EsaR interaction. In addition to stability, EsaR has an inherent fluorescence which becomes quenched in the presence of AHL (Minogue et al, 2002). By first establishing the degree of quenching within the wild type, comparisons to the quenching of EsaR* may help elucidate the importance of the amino acid for the AHL-EsaR interaction.

Materials and Methods

A. Strains, plasmids, and growth conditions

All experiments were performed in *Escherichia coli* Top10. The reporter plasmid used in each study described below contained the *esa* box::*lacZ* within pEXT22 and is referred to as pRNP-*lacZ* (Table 2.1). Wild-type and variant forms of *esaR* generated by error-prone PCR and site-directed mutagenesis, are under the control of the P_{BAD} promoter in pBAD22 and were induced with 0.2% arabinose. Blue/white screening occurred on agar plates containing Luria-Bertani (LB) agar medium, 100 µg/ml ampicillin (Ap100), 50 µg/ml kanamycin (Kan50), 200 µg/ml X-gal, and 0.2% arabinose. Ten µM AHL (3-oxo-C6-L-homoserine lactone), diluted in 100 µl of ethyl acetate, was added to the solidified agar via spreading, and allowed to evaporate prior to plating. Strains for the β-galactosidase assays and western immunoblotting were first grown in LB medium and subsequently subcultured into RM minimal medium (2% casamino acids, 1x M9 salts (10x stock: 128 g/L Na_2HPO_4, 30 g/L KH_2PO_4, 5 g/L NaCl, 10 g/L NH_4Cl), 0.4% glucose, and 0.1 M $MgCl_2$ containing Ap100 and Kan50 when appropriate.

B. Generation of EsaR variants through error-prone PCR

Random mutagenesis of *esaR* was performed under conditions similar to those published by Shafikhani et. al in 1997. Primers were used that directly flank *esaR*; EsaRF anneals to the 5' end of *esaR* and contains an *Eco*RI site (Table 2.2), and EsaRR anneals to the 3' end of *esaR* and contains a *Xba*I site (Table 2.2). Each PCR reaction contained 1x Thermo Poly Buffer (New England Biolabs (NEB), Ipswich, MA), 0.2 mM dATP and dGTP, 1.0 mM dCTP and dTTP, 7 mM $MgSO_4$, 0.3 mM $MnCl_2$, 0.5 µM

Table 2.1. Strains and plasmids used throughout this study

Strain or Plasmid	Relevant Information	References
Strain		
E. coli:		
DH5α	F-Ø80d*lacZ*ΔM15Δ(*lacZYA-argF*)*U169 decR recA1 endAI hsd17 phoA supE44 thi-l gyrA96 relA1*	(Hanahan, 1983)
Top 10	F- *mcrA*Δ(*mrr-hsdRMS-mcrBC*) Ø80d*lacZ*ΔM15 Δ*lac*X74 *deoR recAI araD139* Δ(*ara-leu*)*7697 galU galK rpsL* (Str^r) *endAI nupG*	(Grant et al, 1990)
Plasmids		
pBAD22	Arabinose inducible vector, Ap^r	(Guzman et al, 1995)
pBAD-*esaR*	*esaR* ligated into *Eco*RI sites in pBAD22, 15 bp carry over of pGEM vector	(von Bodman, et al, 2003)
pEXT22	IPTG inducible promoter, Kan^R	(Dykxhoorn et al, 1996)
pRNP-*lacZ*	pEXT22 with the natural promoter region of *esaR* fused to *lacZ*	(D. Schu, unpublished results)
pBAD-mut1[a]	pBAD22 vector with mutagenized *esaR*	This Study
pBAD-mut2[a]	pBAD22 vector with mutagenized *esaR*	This Study
pBAD-mut3[a]	pBAD22 vector with mutagenized *esaR*	This Study
pBAD-mut5[a]	pBAD22 vector with mutagenized *esaR*	This Study
pBAD-mut6[a]	pBAD22 vector with mutagenized *esaR*	This Study
pBAD-mut7[a]	pBAD22 vector with mutagenized *esaR*	This Study
pBAD-mut8[a]	pBAD22 vector with mutagenized *esaR*	This Study
pBAD-mut9[a]	pBAD22 vector with mutagenized *esaR*	This Study
pBAD-mut10[a]	pBAD22 vector with mutagenized *esaR*	This Study
pBAD-mut11[a]	pBAD22 vector with mutagenized *esaR*	This Study
pBAD-mut12[a]	pBAD22 vector with mutagenized *esaR*	This Study
pBAD-mut13[a]	pBAD22 vector with mutagenized *esaR*	This Study

pBAD-mut14[a]	pBAD22 vector with mutagenized *esaR*	This Study
pBAD-mut15[a]	pBAD22 vector with mutagenized *esaR*	This Study
pBAD22-27/9	vector pBAD22 with *esaR* mutated by site-directed mutagenesis at bp 27, aa 9	This Study
pBAD22-76/26	vector pBAD22 with *esaR* mutated by site-directed mutagenesis at bp 76, aa 26	This Study
pBAD22-94/32	vector pBAD22 with *esaR* mutated by site-directed mutagenesis at bp 94, aa 32	This Study
pBAD22-220/74	vector pBAD22 with *esaR* mutated by site-directed mutagenesis at bp 220, aa 74	This Study
pBAD22-222/74	vector pBAD22 with *esaR* mutated by site-directed mutagenesis at bp 222, aa 74	This Study
pBAD22-241/81	vector pBAD22 with *esaR* mutated by site-directed mutagenesis at bp 241, aa 81	This Study
pBAD22-249/83	vector pBAD22 with *esaR* mutated by site-directed mutagenesis at bp 249, aa 83	This Study
pBAD22-281/94	vector pBAD22 with *esaR* mutated by site-directed mutagenesis at bp 281, aa 94	This Study
pBAD22-302/101	vector pBAD22 with *esaR* mutated by site-directed mutagenesis at bp 302, aa 101	This Study
pBAD22-310G/104	vector pBAD22 with *esaR* mutated by site-directed mutagenesis at bp 310G, aa 104	This Study
pBAD22-311/104	vector pBAD22 with *esaR* mutated by site-directed mutagenesis at bp 311, aa 104	This Study
pBAD22-316/106	vector pBAD22 with *esaR* mutated by site-directed mutagenesis at bp 316, aa 106	This Study
pBAD22-398/133	vector pBAD22 with *esaR* mutated by site-directed mutagenesis at bp 398, aa 133	This Study
pBAD22-444/148	vector pBAD22 with *esaR* mutated by site-directed mutagenesis at bp 444, aa 148	This Study
pBAD22-531/178	vector pBAD22 with *esaR* mutated by site-directed mutagenesis at bp 531, aa 178	This Study
pBAD22-607/203	vector pBAD22 with *esaR* mutated by site-directed mutagenesis at bp 607, aa 203	This Study

pBAD22-613/205	vector pBAD22 with *esaR* mutated by site-directed mutagenesis at bp 613, aa 205	This Study
pBAD22-706/236	vector pBAD22 with *esaR* mutated by site-directed mutagenesis at bp 706, aa 236	This Study
pBAD22-728A/243	vector pBAD22 with *esaR* mutated by site-directed mutagenesis at bp 728, aa 243	This Study
pBAD22-728T/243	vector pBAD22 with *esaR* mutated by site-directed mutagenesis at bp 728, aa 243	This Study
pBAD22-734/245	vector pBAD22 with *esaR* mutated by site-directed mutagenesis at bp 734, aa 245	This Study
pSUP102	mobilizable vector plasmid, Cm^r	Simon et al, 1986
pSUP102-*esaR*	*araC*, P_{BAD} promoter, and *esaR* inserted through *Sal*I in reverse orientation within tetracycline gene	This Study

a- for specific amino acid substiutions, see Table 2.3

Table 2.2. Primers used throughout this study

Primer Name	Primer Sequence	Restriction Site
Error-prone PCR		
ESARF	5'CCGGAATTCACCATGTTTTCTTTTTTCC 3'	*Eco*RI
ESARR	5'GCTCTAGATCACTACCTGGC 3'	*Xba*I
Site-directed mutagenesis		
BADVF	5' TAACCTTTCATTCCCAGCGGTCG 3'	None
BADR	5'CTTCTCTCATCCGCCAAAAC 3'	None
BADR500	5' CCCGGCGGATTTGTCCTACTC 3'	None
EsaA27TR	5' CCTTGAAAATCATACAATAACGGATACGCTTC 3'	None
EsaA27TF	5' GAAGCGTATCCGTTATTGTATGATTTTCAAGG 3'	None
EsaC76AR	5' GAAAGTTATCTCCGATGGGTAGTCCGG 3'	None
EsaC76AF	5' CCGGACTACCCATCGGAGATAACTTTC 3'	None
EsaG94AR	5' GGGTAGTCCGGATTACACTTACACTGTTG 3'	None
EsaG94AF	5' CAACAGTGTAAGTGTAATCCGGACTACCC 3'	None
EsaT220CR	5' CTCACGGCCCTTAAACGCACC 3'	None
EsaT220CF	5' GGTGCGTTTAAGGGCCGTGAG 3'	None
EsaT222GR	5' CACGGCCTTGAAACGCACCTC 3'	None
EsaT222GF	5' GAGGTGCGTTTCAAGGCCGTG 3'	None
EsaG241AR	5' CTTCGCCGTTTACCTGGGATG 3'	None
EsaG241AF	5' CATCCCAGGTAAACGGCGAGG 3'	None
EsaT249GR	5' CGTTTGCCTGGGAGGAGAATATTACGC 3'	None
EsaT249GF	5' GCGTAATATTCTCCTCCCAGGCAAACG 3'	None
EsaT281AR	5' GACCTGCGGTACACCAAAATTTTCTC 3'	None
EsaT281AF	5' GAGAAAATTTTGGTGTACCGCAGGTC 3'	None
EsaC302AR	5' CACAAAATTTTCTCTTTATACAAGCAATACAACATCG 3'	None
EsaC302AF	5' CGATGTTGTATTGCTTGTATAAAGAGAAAATTTTGTG 3'	None
EsaT310GR	5' CTTTATCCAAGCAAGACAACATCGTTAACGGC 3'	None
EsaT310GF	5' GCCGTTACCGATGTTGTCTTGCTTGGATAAAG 3'	None
EsaA311CR	5' CCAAGCAATCCAACATCGTTAACGGC 3'	None
EsaA311CF	5' GCCGTTAACGATGTTGGATTGCTTGG 3'	None
EsaA316TR	5' CCAAGCAATACAACTTCGTTAACGGCTTTACC 3'	None

EsaA316TF	5’ GGTAAAGCCGTTAACGAAGTTGTATTGCTTGG 3’	None
EsaA398TR	5’ GGCAACGATCTGACTGCGCTGG 3’	None
EsaA398TF	5’ CCAGCGCAGTCAGATCGTTGCC 3’	None
New444R	5’ GGGCACGATGCATATGCTGCTGATTG 3’	None
New444F	5’ CAATCAGCAGCATATGCATCGTGCCC 3’	None
EsaA531CR	5’ CAGAGCGCGGACCAAACG 3’	None
EsaA531CF	5’ CGTTTGGTCCGCGCTCTG 3’	None
EsaG607AR	5’ CCTATGCTGAGATTGCCACTATTACGGG 3’	None
EsaG607AF	5’ CCCGTAATAGTGGCAATCTCAGCATAGG 3’	None
NEW613R	5’ GCTATTGCGGGCATTTCTGTGAGTAC 3’	None
NEW613F	5’ GTACTCACAGAAATGCCCGCAATAGC 3’	None
EsaG706AR	5’ CAGGCTATCAGACTGGGTATAGAACTGGATC 3’	None
EsaG706AF	5’ GATCCAGTTCTATACCCAGTCTGATAGCCTG 3’	None
EsaG728AR	5’ GATCTTATCAGACAGGCAGCGTCAGA 3’	None
EsaG728AF	5’ GCTGACGCTGCCTGTCTGATAAGATC 3’	None
EsaC728TR	5’ CTTATCAGACTGGCAGCGTCAGCG 3’	None
EsaC728TF	5’ CGCTGACGCTGCCAGTCTGATAAG 3’	None
EsaC734TR	5’ CAGACCGGCAGTGTCAGCG 3’	None
EsaC734TF	5’ CGCTGACACTGCCGGTCTG 3’	None
Protein melting assays		
EsaBox1	5’ ACGTGGACTTAACCTGCACTATAGTACAGGCAAGATGATACT 3’	None
EsaBox2	5’ AGTATCATCTTGCCTGTACTATAGTGCAGGTTAAGTCCACGT 3’	None
Cloning of *esaR* into pSUP102		
SALARACF	5’ GGTGTCGACTTATGACAACTTGACGGCTACAT 3’	*Sal*I

EsaRF and EsaRR, 150 ng/µl of pBAD22-*esaR*-wt (Table 2.1) as the template, and 1.2 µl of *Taq* Polymerase (NEB), brought up to 100 µl with dH_2O. This ratio of chemicals is similar to that of Shafikhani et al. The reaction was then placed under the following conditions: 1 cyle: 94°C for 2 minutes; 15 cycles: 94°C for 30 seconds, 50°C for 30 seconds, 72°C for 30 seconds; 1 cycle: 72°C for two minutes. The product was electrophoresed on a 0.8% agarose gel, and the observed 800 base pair fragment was purified via Qiaquick Gel Extraction Kit (Qiagen, Valencia, CA) as suggested by the manufacturer.

A double digestion using the enzymes *Eco*RI and *Xba*I was performed on both the mutated *esaR* PCR product and the vector pBAD22 (Table 2.2) for 2 hours at 37°C. The vector and insert were then ligated together using T4 DNA ligase (NEB) for 2 hours at 25°C as stated in the manufacturer's directions. Transformations into an *E. coli* Top10 strain with pRNP-*lacZ* (Table 2.1) then occurred through the heat shock treatment of competent cells (see below). The cells and DNA were combined with 0.1 M $CaCl_2$ for 15 minutes, heat shocked at 37°C for 2 minutes, and placed on ice for 5 minutes. Afterwards, the cells were grown in LB broth for 45 minutes with shaking and were subsequently plated for blue/white screening with the appropriate antibiotics.

C. Generating competent cells

In order to make competent cells, overnight cultures were grown from freezer stocks in 5 ml LB. The following morning the culture was subcultured to an OD_{600} of 0.05 into 5 ml of LB and allowed to grow until an OD_{600} of 0.5 was reached. The cells were chilled on ice for approximately 30 minutes and subsequently centrifuged in a refrigerated centrifuge for 10 minutes at 5,000 rpm. The supernatant was discarded and

the pellet was resuspended with 1 ml of 0.1 M $MgCl_2$, followed by centrifugation for 10 minutes at 5,000 rpm. The resulting cell pellet was resuspended in 1 ml of 0.1 M $CaCl_2$ and incubated on ice for 30 minutes. The cells were recentrifuged for 10 minutes at 5,000 rpm and the supernatant was discarded. The pellet was resuspended once again in a mixture of 212 µl $CaCl_2$ plus 38 µl of 100% glycerol and frozen in 50 µl aliquots at -80ºC.

D. Screening for *esaR* mutants that no longer respond to AHL

The transformed *E. coli* Top10/pRNP-*lacZ* strain contains two plasmids; pBAD22 encoding mutagenized *esaR* and pRNP-*lacZ* (Table 2.1). In the presence of wild-type EsaR, the transcription of *lacZ* from the reporter plasmid will be repressed. Expression of the reporter becomes derepressed after the wild-type EsaR complexes with the AHL. Therefore, when the AHL is present, the colonies encoding wild-type EsaR will appear blue when plated on X-gal. The desired phenotype are white colonies. This demonstrates that a variant form of EsaR is being produced that no longer responds normally to the AHL, constitutively repressing transcription of *lacZ*.

Variant white colonies were patched onto plates for blue/white screening along with the positive control, *E. coli* Top10/pBAD22-wt *esaR* /pRNP-*lacZ*. The patched colonies that remained white in the absence and presence of AHL were grown up overnight in 5 ml LB, Ap100 and Kan50 and were purified using a Qiaprep Miniprep Kit. Plasmids (50 ng/µl) and the primers BADVF and BADR (5 pmol/µl) (Table 2.2) which anneal to the pBAD22 vector 500 bp upstream the start of *esaR*, and 43 bp downstream *esaR* respectively were given to the Core DNA Sequencing Facility at Virginia's

Bioinformatics Institute, Virginia Tech, Blacksburg, VA (CSF-VBI) to determine the nucleotide sequence of the mutated genes.

E. β-galactosidase assay

β-galactosidase assays were performed in order to quantify LacZ levels. Strains were grown for approximately 7 hours in Ap100 and Kan50 and subcultured overnight in the absence of arabinose at 30°C in RM minimal medium. The following morning, the *E. coli* Top10/pBAD22-*esaR**/pRNP-*lacZ* strain was subcultured to an OD_{600} of 0.05 in 5 ml of the same medium under two different conditions: (a) with 20 μM 3-oxohexanoyl-L-HSL and 0.2% arabinose or (b) with 0.2% arabinose only, and grown to an OD_{600} of 0.5. At this point, 5 μl aliquots were stored at -70°C. β-galactosidase assays were then performed using a chemiluminescent reporter assay kit (Tropix, Bedford, MA) and a Beckman Coulter LD 400 microplate reader (Beckman Coulter, Fullerton, CA). The procedure for β-galactosidase assays was provided by the manufacturer. The β-galactosidase assays for the site-directed generated variants differed from those of error-prone PCR generated variants, as actively growing cells were induced with 0.02% arabinose at an OD_{600} of 0.1 as opposed to being induced upon subculturing.

F. EsaR* variant stability determined through western blot.

E. coli Top10 strains encoding wild-type EsaR as well as the variants of interest were grown overnight from freezer stocks in 5 ml LB. The following morning the cells were subcultured to an OD_{600} of 0.05 and allowed to grow at 30°C. At an OD_{600} of 0.25, arabinose was added to the growing culture to induce the production of the protein. Once an OD_{600} of 1.0 was reached, aliquots of 1 ml were transferred to an eppendorf tube and the cells were pelleted through centrifugation. The supernatant was decanted, and the

pellet was frozen at -70°C. The pellets were then allowed to thaw at room temperature, and subsequently diluted in 100 µl in 1x sample buffer (from 5x sample buffer: 1 M Tris pH 6.8, 0.2 g SDS, 0.625 g glycerol, 0.5 ml β-mercaptoethanol, trace bromophenol blue (BPB) per 3 ml) and boiled for 3 minutes prior to loading on duplicate 15% SDS-polyacrylamide gels. A kaleidoscope standard (Bio-Rad, Hercules, CA) was used unaltered and 10 µl was loaded next to the other samples. The gels were electrophoresed for approximately 1.5 hours at 150 V. After completion, one gel was stained for total protein expression via Coomasie Brilliant Blue (Bio-Rad), while the proteins on the second gel were transferred to a nitrocellulose membrane for 1 hour at 100V using the BioRad Mini-Protean® 3 Electrophoresis Module. After the transfer, the nitrocellulose membrane was treated with 1x NET buffer (150 mM NaCl, 5mM EDTA, 54.6 mM Tris-HCl, 8 mM Tris-Base, 500 µl Triton X-100 per liter), with the addition of 0.25% w/v of gelatin as the blocking buffer, and incubated with shaking for 1 hour at room temperature. This buffer was combined with the 1° antibody (polyclonal anti-*esaR*) in a working dilution of 1:500, and allowed to incubate with the nitrocellulose for approximately 1 hour at room temperature. After incubation, the 1° antibody was removed and stored at -20°C for future use. The blot was washed for 10 minutes in fresh 1x NET buffer, 3 times. It was then incubated with the 2° antibody, horseradish peroxidase-conjugated goat IgG fraction to rabbit IgG (ICN, Aurora, OH) in a 1:2000 dilution, with the 1x NET buffer as the dilutent for approximately 1.5 hours. The 2º antibody solution was removed, and the blot was incubated in 100 ml of 50 mM Tris pH 7.5 for 12.5 minutes. While incubating, the color developing agents were prepared. 4-Cholor-1-napthol (0.06 g) was dissolved in 20 ml of methanol. Additionally, 83 µl of 3%

hydrogen peroxide was added to 100 ml of 50 mM Tris (pH 7.4). At the end of the 12.5 minute incubation the solution was decanted, and the two coloring reagents were poured over the blot simultaneously and the blot was incubated in the dark until a strong banding pattern appeared. The reaction was stopped with the addition of dH_2O.

G. Mutational mapping onto the EsaR homology model

A crystal structure of EsaR has not yet been obtained. However, a homology model of EsaR based on the crystal structure of TraR (Zhang et al, 2002) is available, and has kindly been provided by A. Thode, D. Donham, and M. Churchill. The model relies heavily on TraR to orient the folding patterns of the N-terminal and C-terminal domains of EsaR. The biochemical properties of the AAs were used to find the appropriate folding pattern for the elongated linker region and extended C-terminal region, as these features are unique to LuxR-type repressors. Using this homology model, the amino acid substitutions identified by sequencing have been plotted onto EsaR with the protein modeling program PyMOL, using the commands outlined in the program guidelines. This may help to visualize a potential binding pocket/region within EsaR for the AHL.

H. Site-directed mutagenesis

As sequencing has shown, there are several variants that have multiple mutations in *esaR* (Table 2.3). In order to determine which of the several mutations is responsible for producing the desired AHL-nonresponsive phenotype, the mutations needed to be dissected apart. Forward and reverse primers for each mutation were ordered from IDT DNA (Coralville, IA) that contained the base pair substitution in the center of the primer, and approximately ten to fifteen base pairs on either side of the mutation (Table 2.2).

Table 2.3. A comprehensive list of mutations achieved in error-prone PCR and the resultant amino acid changes

Mutant Strain Name	Codon Change	Base Pair Change	Amino Acid Substitution	Polarity/Charge Change
MUT1	CAA → CAT	27[b]	Gln9 → His9	Polar (0) → Polar (+)
	GCT → ACT	94[b]	Ala32 → Thr32	Nonpolar (0)→ Polar (0)
	CCG → TTG	728T[b]	Pro243 → Leu243	No change
MUT2	TTC → TAC	296	Phe98 → Tyr98	Nonpolar (0) → Polar (0)
MUT3	TTT → CTT	220[b]	Phe74 → Leu74	Nonpolar (0) → Nonpolar (0)
	TAC → GAC	310G[b]	Tyr104 → Asp104	Polar (0) → Polar (-)
	CAG → CAT	444[b]	Gln148 → His148	Polar (0) → Polar (+/0)
MUT4[a]	TCC → TAC	302[b]	Ser101 → Tyr101	Polar (0) → Polar (0)
MUT5	GCT → GTT	95	Ala32 → Val32	Nonpolar (0) → Nonpolar (0)
MUT6	TCC → CCC	301	Ser101 → Pro101	Polar (0) → Nonpolar (0)
MUT7	GCC → ACC	241[b]	Ala81 → Thr81	Nonpolar(0) → Polar(0)
	ATC → TTC	316[b]	Ile106 → Phe106	No change
MUT8	TAC → AAC	310A	Tyr104 → Asn104	No change
MUT9	TTC → TAC	296	Phe98 → Tyr98	Nonpolar(0) → Polar(0)
MUT10	TTT → TTG	222[b]	Phe74 → Leu74	No change
	TAC → TCC	311[b]	Tyr104 → Phe104	Polar (0) → Nonpolar (0)
	CAG → CTG	398[b]	Gln133 → Leu133	Polar(0) → Nonpolar (0)
MUT11	TTC → TAC	281[b]	Phe94 → Tyr94	Nonpolar (0) → Polar (0)
	TTC → TAC	296	Phe98 → Tyr98	Nonpolar (0) → Polar (0)
MUT12	GCC → ACC	241	Ala81 → Thr81	Nonpolar (0) → Polar (0)
	ATC → TTC	316	Ile106 → Phe106	No change
MUT13	TTC → TAC	281	Phe94 → Tyr94	Nonpolar (0) → Polar (0)
	TTC → TAC	296	Phe98 → Tyr98	Nonpolar (0) → Polar (0)
MUT14	CTG → ATG	76[b]	Leu26 → Met26	No change
	GAT → GAG	249[b]	Asp83 → Glu83	No change
	TCC → CCC	301	Ser101 → Pro101	Polar (0) → Nonpolar (0)
	AAA → CAA	531[b]	Lys178 → Gln178	Polar (+) → Polar (0)
	GTA → ATA	706[b]	Val236 → Ile236	No change
	GCG → GTG	734[b]	Ala245 → Val245	No change
MUT15	TTC → TAC	296	Phe98 → Tyr98	Nonpolar (0) → Polar (0)
	GCT → ACT	607[b]	Ala203 → Thr203	Nonpolar (0) → Polar (0)
	ACG → GCG	613[b]	Thr205 → Ala205	Polar (0) → Nonpolar (0)
	CCG → CAG	728A[b]	Pro243 → Gln243	Polar (0) → Nonpolar (0)

a- Mut 4 was unable to sequenced properly in both orientations. The mutation initially observed from partial sequence in the reverse orientation was re-achieved through site-directed mutagenesis.
b- amino acid substitutions regenerated in isolation via site-directed mutagenesis.

Primers were resuspended to a final concentration of 50 μM. To amplify the 5' end of the gene mutational primers binding to the middle of *esaR* were used in conjunction with BADVF, which anneals at the 5' end 500 base pairs upstream of *esaR* in the vector pBAD22. Each reaction contained: 500 nM mutational 5' primer, 500 nM BADVF, 1x Thermo Poly Buffer, 200 μM dNTPs, 1 unit Deep Vent (NEB), and 100 ng/μl of template pBAD22-wt-*esaR*, brought up to 50 μl using dH_2O. A standard PCR protocol then ensued with the following conditions: 1 cyle: 95°C for 2 minutes; 29 cycles: 95°C for 30 seconds, temperature from Table 2.4 for 1 minute, 75°C for 1 minute 15 seconds; 1 cycle: 75°C for 10 minutes. Modifications of the standard PCR reaction were necessary to obtain various forward directional gene mutations, and can be viewed in Table 2.4. The method to obtain the 3' end of *esaR* was similar to that described above for the 5' end. Mutational 3' primers annealed at the middle of the gene and were used in combination with primers BADR or BADR500 (Table 2.2), which anneal at the 3' end 43 base pairs and 500 base pairs respectively downstream the C-terminal end of *esaR* in pBAD22. 3' end mutational fragments 27, 76, 94, 220, 222, 241, 249, 302, 310, 316, 398, 532, and 607 were created with BADR while 3' end fragments 311, 444, 613, 706, 728, and 734 used primer BADR500. Each reaction consisted of the following reagents: 500 nM mutational 3' primer, 500 nM BADR or BADR500, 1x Thermo Poly Buffer, 200 μM dNTPs, 1 unit Deep Vent (NEB), 100 ng/ μl template pBAD22-wt-*esaR*, brought up to 50 μl with dH_2O. The thermocycler was programmed as follows: 1 cyle: 95°C for 2 minutes; 29 cycles: 95°C for 30 seconds, temperature from Table 2.4 for 1 minute, 75°C for 1 minute 15 seconds; 1 cycle: 75°C for 10 minutes. Modifications to the standard PCR mix

Table 2.4. Protocol deviations for the first round of PCR in site-directed mutagenesis

Mutation/ Substitution	Changes Made to Protocol
27/9	BADR[a], R=55 ºC[b], F=55 ºC[c]
76/26	BADR[a], R=58.3ºC[b], F=57.3 ºC[c]
94/32	BADR[a], R=57 ºC[b], F=57 ºC[c]
220/74	BADR[a], R= 59 ºC[b], F=57 ºC[c]
222/74	BADR[a], R=59 ºC[b], F=57 ºC[c]
241/81	BADR[a], R=58 ºC[b], F=57 ºC[c]
249/83	BADR[a], R=59.1 ºC[b], F=57.3 ºC[c]
281/94	BADR[a], R=56.4 ºC[b], F=56.4 ºC[c]
302/101	BADR[a], R=55 ºC[b], F=56 ºC[c]
310G/104	BADR[a], R=59.6 ºC[b], F=58 ºC[c]
311/104	BADR500[a], R=59 ºC[b], F=57.9 ºC[c], 600 nM primers
316/106	BADR[a], R=59.5 ºC[b], F=58 ºC[c]
398/133	BADR[a], R=61.5 ºC[b], F=58 ºC[c]
444/148	BADR500[a], R=58 ºC[b], F=57 ºC[c]
531/178	BADR[a], R=58.1 ºC[b], F=58.1 ºC[c]
607/203	BADR[a], R=58.4 ºC[b], F=57.3 ºC[c]
613/205	BADR500[a], R=58 ºC[b], F=57.5 ºC[c]
706/236	BADR500[a], R=57 ºC[b], F=57 ºC[c], 700 nM primers, 200 ng/µl template
728A/243	BADR500[a], R=57 ºC[b], F=57 ºC[c], 700 nM primers, 200 ng/µl template
728T/243	BADR500[a], R=57 ºC[b], F=57 ºC[c], 700 nM primers, 200 ng/µl template
734/245	BADR500[a], R=57 ºC[b], F=57 ºC[c], 700 nM primers, 200 ng/µl template

a- denotes the reverse primer used in the PCR reaction
b-annealing temperature for the 5' PCR reaction
c-annealing temperature for the 3' PCR reaction

and reaction were necessary to obtain the reverse fragment, and can be viewed in Table 2.4.

Once the two first-round PCR reactions were complete for each respective base pair mutation, the products were electrophoresed on a 0.8% agarose gel. Bands that met the appropriate size criteria were excised from the gel and purified using Qiaquick Gel Extraction Kit (Qiagen) as suggested by the manufacturer. The DNA was quantified using a UV-Visible spectrophotometer (Thermo Spectronic, Cambridge, Great Britain). Using these fragments, a second round of PCR was performed in order to obtain a full length *esaR* gene containing the mutation. The 5' and 3' fragments of *esaR* overlap in length by the number of base pairs in the mutational primers used to generate the fragment. The reaction mixtures consisted of the following: 2 µM BADR or BADR500, 2 µM BADVF, 200 µM dNTPs, 1x Thermo Poly Buffer, 100 ng/µl of the 5' *esaR* fragment, 100 ng/µl of the 3' *esaR* fragment, and 1 unit Deep Vent (NEB) brought up to 50 µl with dH_2O. The PCR reaction was programmed for: 1 cyle: 95°C for 2 minutes; 29 cycles: 95°C for 30 seconds, temperature from Table 2.5 for 1 minute, 75°C for 1 minute 30 seconds; 1 cycle: 75°C for 10 minutes.

Upon completion of the second round of PCR, the full length *esaR** gene and the vector pBAD22 were digested with both *Nhe*I and *Hind*III for 2 hours at 37ºC. The double digestion reactions were inactivated at 65 ºC for 20 minutes and subsequently ligated together for 2 hours at room temperature. Each of the ligation reactions were transformed separately into *E. coli* Top10/pRNP-*lacZ*. Blue/white screening and β-galactosidase assays were used to determine specific amino acid residues that are involved in the EsaR-AHL interaction, and those that are not.

Table 2.5. Annealing temperatures used in second round PCR reactions for site-directed mutagenesis.

Mutation/ Substitution	Annealing temp. of primer to first round PCR fragments	Mutation/ Substitution	Annealing temp. of primer to first round PCR fragments
27/9	56ºC	316/106	58ºC
76/26	57.3ºC	398/133	58ºC
94/32	57.3 ºC	444/148	57ºC
220/74	58 ºC	531/178	58.1ºC
241/81	57 ºC	607/203	58.3ºC
222/74	58 ºC	613/205	57.5ºC
249/93	57.3 ºC	706/236	57ºC
281/94	56.4ºC	728A/243	57ºC
302/101	56ºC	728T/243	57ºC
310G/104	58ºC	734/243	57ºC
311/104	57.9ºC		

I. Separating plasmids

In generating the initial variant strains, PCR fragments were ligated into pBAD22 and transformed into a strain which already contained the reporter plasmid. Therefore, it was necessary to separate out these plasmids for protein work and other genetic experiments. Cells were grown up overnight in Ap100, omitting Kan50, and the plasmid was isolated using the Qiaprep Miniprep Kit as suggested by the manufacturer, with the following modifications: 1 ml of cells were centrifuged for plasmid isolation, and the plasmid was eluted in 100 µl of dH_2O. One microliter of the diluted plasmid was then chemically transformed into *E. coli* Top10. Approximately 100 of the resultant colonies were patched onto two plates, one containing Kan50 followed by a plate containing Ap100. One colony per variant with the ability to grow on ampicillin but unable to grow on kanamycin was chosen to make freezer stocks.

J. Dominant negative assays

Work has been completed on a dominant negative genetic assay on the EsaR* variants of interest. When a plasmid encoding mutagenized *esaR* is transformed into a strain containing a plasmid encoding wild-type EsaR, three EsaR complexes are predicted: wild-type homodimers, variant homodimers, or heterodimers composed of EsaR and EsaR*. If the EsaR* are indeed "loss of function", then they should be dominant over EsaR in the presence of AHL.

For these assays, *E. coli* Top10 cell strains will contain three separate plasmids: the reporter plasmid pRNP-*lacZ*, mutated *esaR* within pBAD22, and *esaR*-wt cloned into pSUP102 (Table 2.1). In order to construct pSUP102-*esaR*-wt, a fragment containing *esaR* downstream of the P_{BAD} promoter and *araC*, was amplified from pBAD22-*esaR*-wt

using PCR. A primer was created which anneals to the 5' end of *araC* with a *Sal*I sequence overhang (SALARACF) and the 3' end of *esaR* was amplified using the previously described BADR (Table 2.2). The PCR reaction contained 500 nM SALARACF, 500 nM BADR, 1x Thermo Poly Buffer, 200 μM dNTPs, 1 unit Deep Vent (NEB), 100 ng/μl of template pBAD22-wt-*esaR*, and was brought up to 50 μl using dH_2O. The thermocycler was set for the following cycles: 1 cyle: 95°C for 2 minutes; 29 cycles: 95°C for 30 seconds, 60.2°C for 1 minute, 75°C for 1 minute 35 seconds; 1 cycle: 75°C for 10 minutes. A polyA tail was added to the ends of the PCR fragment for ligation into pGEM-T easy vector (Promega, Madison, WI) as suggested by the manufacturer using *Taq* Polymerase (NEB). The PCR fragment was ligated into pGEM-T according to Promega, chemically transformed into *E. coli* Top10, and plated onto agar containing Ap100, 200 μg/ml X-gal, and 80 μg/ml IPTG. Resultant white colonies may indicate that the PCR fragment was properly inserted into the *lacZ* gene of pGEM-T, thus rendering it nonfunctional. These colonies were subsequently grown overnight in 5 ml LB and Ap100, and plasmid purification using the Qiaprep Miniprep Kit ensued. The plasmids were then subjected to a restriction digestion using *Sal*I, to verify the presence of the fragment. Additionally, a PCR reaction was performed in which the reaction conditions were identical to that as described above, differing only in the template used (pGEM-T/PCR fragment), to verify the presence of the insert. Those strains containing plasmids with the correct 1.8 Kb were given to CSF-VBI for confirmation of the PCR fragment sequence.

The 1.8 Kb fragment, which was gel purified from the digestion confirmation above, was ligated into pSUP102 that had previously been digested with *Sal*I, followed

by heat inactivation of the enzyme for 20 minutes at 65ºC. The ligation mixture of the PCR fragment and the vector pSUP102 was subsequently transformed into competent *E. coli* Top10. Proper fragment insertions were verified via phenotype screening for the loss of tetracycline resistance. The insertion occurs within the tetracycline gene, hence disrupting it. To ensure that the regulation of *esaR* was under the control of P_{BAD} and not the tetracycline resistance gene promoter, restriction mapping using the enzymes *Kpn*I and *Nco*I ensued. Once the correct pSUP102-*esaR*-wt constructs were verifed, it was subsequently transformed into *E. coli* Top10/pRNP-*lacZ*.

To make certain that the wild type gene was being expressed and functional, a β-galactosidase assay was performed in the presence and absence of AHL. Once considered to be constructed correctly, the resulting strain was made into competent cells. Competent *E. coli* Top10/pRNP-*lacZ*/pSUP102-*esaR* were then transformed with the pBAD22-*esaR** vectors. These strains were subsequently stored as freezer stocks, and subjected to β-galactosidase assays (see above). A negative control strain containing pRNP-*lacZ* and empty vectors pSUP102 and pBAD22, and a positive control containing pRNP-*lacZ*, pSUP102-*esaR*-wt, and the empty vector pBAD22 were created as well.

K. Purification of EsaR

In order to test the affinity of EsaR* for AHL, the degree of affinity for the wild-type must be first established. It was therefore necessary to purify the protein through the aid of the polyhistidine-tag (His) and the maltose binding protein (MBP), added to the N-terminal domain of *esaR*. The His-MBP-EsaR fragment is expressed from the P_{lac} promoter in *E. coli*. This strain was grown overnight from a freezer stock in 5 ml of LB broth and Ap100 at 30ºC. The following morning, the entire 5 ml of culture was

subcultured into 100 ml of LB with Ap100 and grown to an OD_{600} of 0.6, at which point it was induced with 1 mM of IPTG. After induction, the flask was transferred to a refrigerated shaker, where it was allowed to shake at 19ºC overnight. Cells from this overnight culture were maintained on ice during processing, ensuring that the stability of EsaR was not compromised. The cells were centrifuged using the Beckman Coulter centrifuge (Brea, CA) with the Ja-16.25 rotor for 10 minutes at 10,000 rpm. After discarding the supernatant, the cell pellet was resuspended in 10 ml of DS buffer (50 mM Tris (pH 7.5), 10% glycerol, 500 mM NaCl, 10 mM imidazole), and passed through a French press at 9,000 psi three times. The cell lysate was aliquoted into microcentrifuge tubes and centrifuged at 14,000 g for 30 minutes at 4ºC. Subsequently, the supernatant was combined with 1 ml of Ni-NTA agarose beads (Qiagen) in a 15 ml conical tube and allowed to shake for approximately 1 hour at 4ºC. The Ni-resin-supernatant mixture was then added to a column, and the flowthrough was collected into a 10 ml conical tube. The resin was washed twice, each with 10 ml of wash buffer (20 mM Tris (pH 7.5), 500 mM NaCl, 10% glycerol, 20 mM imidazole), and with 1 ml of elution buffer (20 mM Tris (pH 7.5), 500 mM NaCl, 10% glycerol, 250 mM imidazole), for 3 repetitions. The 3 ml of elutant collected was added to a conical tube containing 1 ml of amylose resin that had previously been washed in 10 ml of wash buffer. The elution-amylose mixture was shaken for 1 hour at 4ºC. The column was washed of the Ni-NTA beads, and after the 1 hour was complete the elution-amylose resin mixture was added; the flowthrough was collected in a 15 ml conical tube. The amylose beads were washed twice, each with 10 ml, of TNG buffer (20 mM Tris (pH 7.5), 500 mM NaCl, 10% glycerol), and the protein was eluted three separate times with 1 ml of TNG buffer + 10 mM maltose.

Throughout the washes and elutions, samples were taken at each of the following steps: 10 µl for the post-lysis, flowthroughs, and elutions, and 300 µl for each wash. These samples were then analyzed using a 15% SDS-PAGE gel, in order to determine the relative purity of His-MBP-EsaR.

L. Protein quantification using the Bradford assay

Starting with 500 µg/ml of BSA mixed with dye reagent (Bio-Rad, Richmond, CA) and dH_2O, a 1:2 dilution standard curve was established in which the BSA concentration ranged from 500 µg/ml to 3.9 µg/ml. For His-MBP-EsaR, a 1:200 dilution was created by adding the dye and water (795 µl dH_2O and 200 µl dye) to the protein. The filter of the spectrophotometer (Spectronic 2D+, Miller Roy, Canada) was set to a wavelength of 595 nm. The absorbance of the standard curves was measured in increasing BSA concentration, measuring the absorbance of His-MBP-EsaR once the BSA concentration of 16.25 µg/ml was recorded. When the spectrophotometer reached an OD_{595} of 1.0, samples were no longer read as the spectrophotometer becomes inaccurate due to light scattering. The µg concentration of the BSA dilutions was plotted against the OD_{595} values measured using Microsoft Excel, and the equation of the best fit line was generated. Substituting the OD_{595} of the protein sample for y, x was solved for in order to determine the concentration of His-MBP-EsaR in µg/ml.

M. Determining protein concentration using a spectrophotometer

After protein purification was achieved, the molar concentration was determined through measuring the absorbance of the protein at A_{280} using the UV-Visible spectrophotometer. The absorbance was divided by the molar extinction coefficient (99240 M^{-1} cm^{-1}) for EsaR, found by entering in the entire protein sequence in ExPASy

using the following link: http://ca.expasy.org/cgi-bin/protparam. To determine the concentration in mg/ml, the value obtained by division was multiplied by the molecular weight.

N. Protein melting assay

As observed by Minogue et al in 2002, the thermal stability of EsaR increases in the presence of the AHL, 3-oxo-C6-L-homoserine lactone. This attribute can therefore be utilized in determining the degree of affinity of EsaR* for the AHL after a base-level of affinity or stability is first determined for EsaR. An RT-PCR thermocycler has been programmed to increase in temperature over time, causing the protein to unfold at a critical temperature. When the protein is denatured in the presence of the dye SYPRO-ORANGE, it will bind to the hydrophobic regions of the denatured protein and fluoresce, which is subsequently read by the RT-PCR thermocycler. These values are then exported to Microsoft excel which contains the downloaded software feature XLFit. The data are best fit to a regression curve, and its inflection point is the Tm of the protein, or its thermal stability, thus demonstrating the affinity of the protein for the AHL.

A new file was created in the RT-PCR thermocycler which applied the dye sypro-green, pre-programmed in the software, to all wells containing samples. Within the tab titled instrument area, the last stage was deleted, making sure two stages were left. To the last stage, a second step was added. The temperature was set to 10ºC for the first stage. Within the second stage, the first step was assigned as 10ºC for 1 second, while the second step was set to 11ºC for 1 minute. Additionally, at the top of the program screen, the repetition was changed to 85. Furthermore, under the auto-increment tab, it was ensured that 1ºC was entered for each step in the second stage and the sample

volume was changed to 30 µl. Lastly, under the "data collect" tab, the data collection was set to collect from stage two, step two.

In order to determine the maximum concentration of AHL that His-MBP-EsaR will respond to, a dilution scheme was performed in which the AHL concentration varied from 100 nM to 100 µM. Samples were prepared in triplicate in a 96-well plate, and the ethyl acetate was allowed to evaporate, leaving behind the AHL. A series of master mixes was assembled accounting for either the controls: AHL only, DNA only, EsaR only, EsaR and AHL, EsaR and DNA, or the experimental setup, EsaR and DNA with varying concentrations of AHL. For those reactions that did not contain protein or DNA, a master mix of 50x SYPRO-ORANGE, 150 mM NaCl, and 100 mM Hepes, brought up to 25 µl with dH_2O was assembled. A master mix of 50x SYPRO-ORANGE, 150 mM NaCl, 100 mM Hepes, and 25 µM DNA brought up to 25 µl with dH_2O was created for reactions that contained DNA only, and 50x SYPRO-ORANGE, 150 mM NaCl, 50 mM Hepes, 25 µM DNA brought up to 25 µl with dH_2O was mixed for reactions with DNA and protein. Each master mix was added appropriately to water or 5 µg/µl of protein to bring the reaction up to 30 µl and added to the 96-well plate in triplicate. At the conclusion of the cycles, the data was exported into XLFit and a Tm was established as previously described.

O. Fluorescence Spectroscopy

A second way in which the affinity of EsaR and its variants for the AHL can be determined is through fluorescence spectroscopy. EsaR contains an intrinsic fluorescence which is quenched upon AHL binding due to three tryptophan residues (Minogue et al, 2002). By first establishing "normal" quenching with the wild type, the

amount of quenching found within variant strains can help determine this affinity for the AHL. A RF-1501 spectrofluorometer (Shimadzu, Columbia, MD) was used to perform a scan of the protein at a concentration of 370 nM in order to establish an emission wavelength and an excitation wavelength. Once obtained, the values were entered into the program and the fluorescence intensity of EsaR was measured.

Results and Discussion

Generating and screening variants

The error-prone PCR reactions used to generate EsaR* variants contained $MnCl_2$. This caused the fidelity of *Taq* polymerase to decrease, permitting misincorporation of various nucleotides. A concentration of 0.3 mM $MnCl_2$ was experimentally determined to yield enough PCR product to produce a visible band within a 0.8% agarose gel (data not shown). At this concentration *Taq* polymerase was able to generate 1 to 7 mutations per gene. If the $MnCl_2$ concentration was in the range of 0.3 mM to 0.5 mM, then the DNA polymerase activity was greatly inhibited, and failed to yield a PCR product. Concentrations below 0.3 mM $MnCl_2$ were not tested as 0.3 mM proved successful in generating mutations. As well as adding this extra component to the PCR reactions, the number of cycles used for step 2 (see Materials and Methods) was reduced to 16. This helped decrease the number of mutations per gene, as one base pair substitution per gene was considered ideal.

After directly cloning the mutated fragment into pBAD22 and subsequently transforming the resulting plasmid into *E. coli* Top10/pRNP-*lacZ*, screening for the desired mutants occurred. A recognizable mutant appeared white during blue/white screening in the presence of AHL. This indicated that the variants were no longer able to respond properly to the AHL signal, becoming non-inducible and blocking the transcription of the *lacZ* gene. A total of 14 variant strains have been identified by screening as well as β-galactosidase assays, which helped to further confirm a loss of responsiveness towards the AHL (Figure 2.1). These variants contained

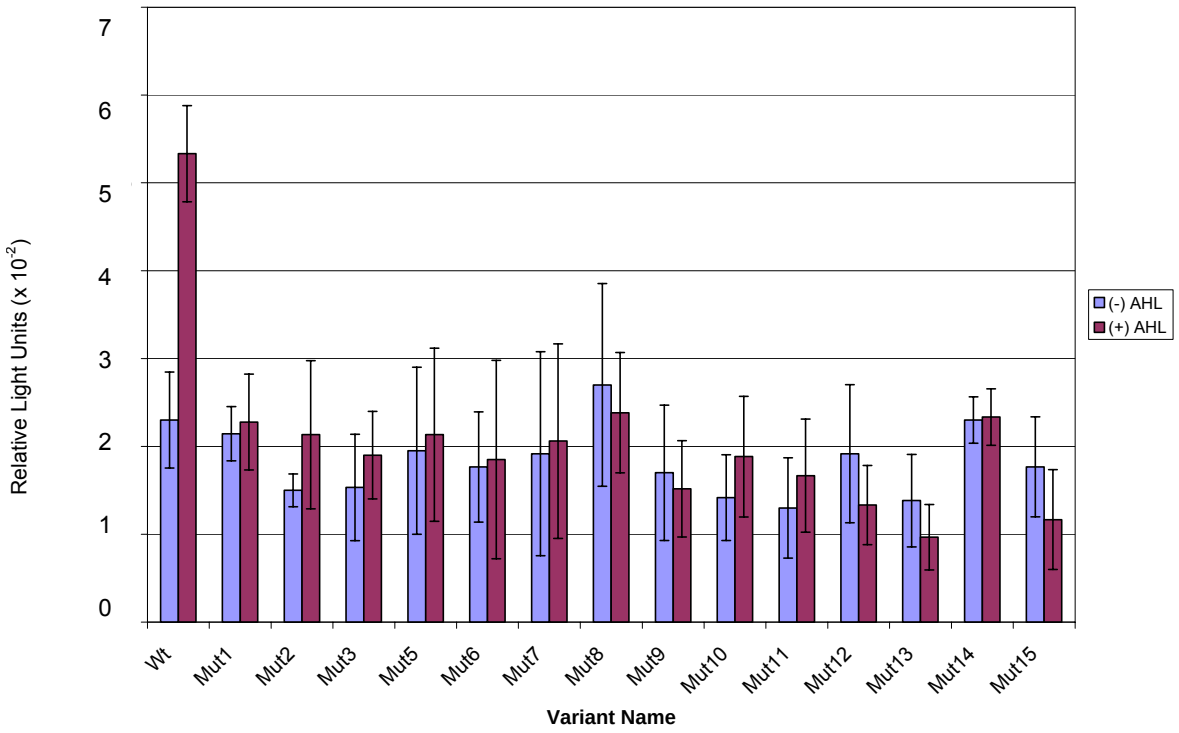

Figure 2.1. Confirming the variants loss of responsiveness to AHL through repression assays. β-galactosidase assays were performed as described in the text with pBAD-*esaR* wild-type or pBAD-mut1-15. Samples from two independent experiments were tested in triplicate, with error bars representing the standard deviation of the data generated. The pBAD-*esaR* in the presence of AHL has a two-fold activation in contrast to pBAD-*esaR* in the absence of AHL, and pBAD-mut1-15 with or without the AHL.

comparable levels of β-galactosidase activity in the presence of AHL as the wild type in the absence of AHL (Figure 2.1).

Although it is known that EsaR* is present and retains its DNA binding functionality through the repression assays, a western blot was performed, nonetheless, in order to verify the stability of the variants and to help determine a relative quantity of EsaR* produced (Figures 2.2; 2.3). All variants were confirmed to be stable; the amount of EsaR* protein produced from the various strains was qualitatively similar.

Analysis of mutations obtained

Sequencing of the 14 original EsaR* variants has revealed a total of 25 distinct mutations which result in 24 individual amino acid substitutions, scattered throughout the protein (Table 2.3; Figure 2.4). These substitutions can be divided into three different categories: amino acid substitutions in which (1) the charge changes, (2) polarity changes, and (3) the amino acid properties are similar. Chemical-property changes within the substituted residues account for 56% of the total amino acid substitutions. These chemically changed residues may result in (1) structural changes causing the AHL binding pocket to refold in a manner such that amino acids critical for AHL binding are no longer available, (2) conformational changes may cause the binding pocket to disappear altogether, (3) these side chain substitutions may affect the EsaR-AHL binding, in that the atoms needed for van der Waals interactions or for hydrogen bonding are no longer present, preventing a stable interaction from occurring, (4) different amino acids may cause steric hindrance between the AHL and the binding pocket, (5) the protein may misfold such that it becomes locked into a conformation that no longer responds to AHL, and (6) the propagation of the signal from the N-terminal domain to the C-terminal

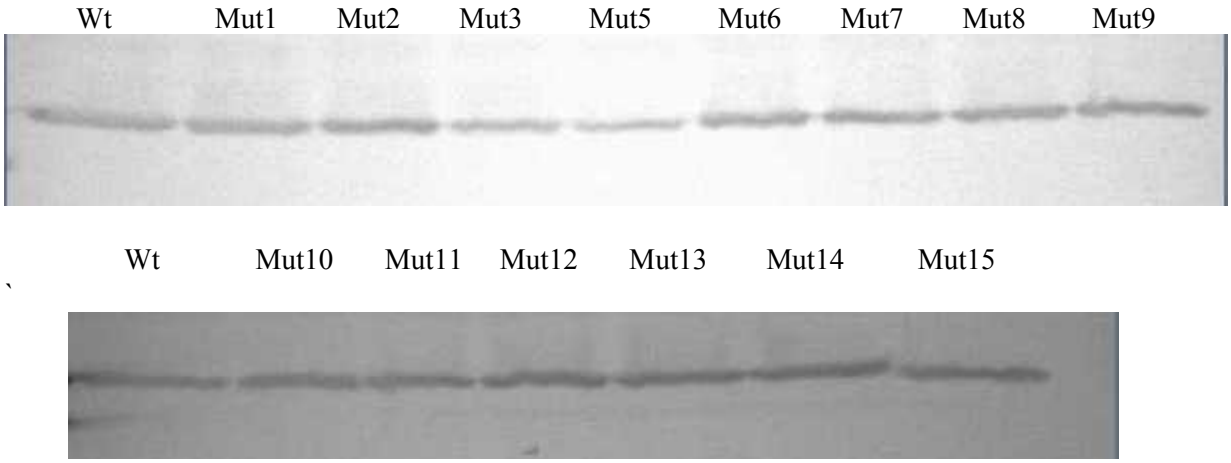

Figure 2.2. Western blots demonstrating the stability and relative quantity of EsaR* variants. The 28 kDa EsaR band was visualized with anti-EsaR antibody. The negative control is the wild-type protein uninduced with arabinose, and the positive control is the wild-type EsaR induced by arabinose. Each blot was performed in duplicate.

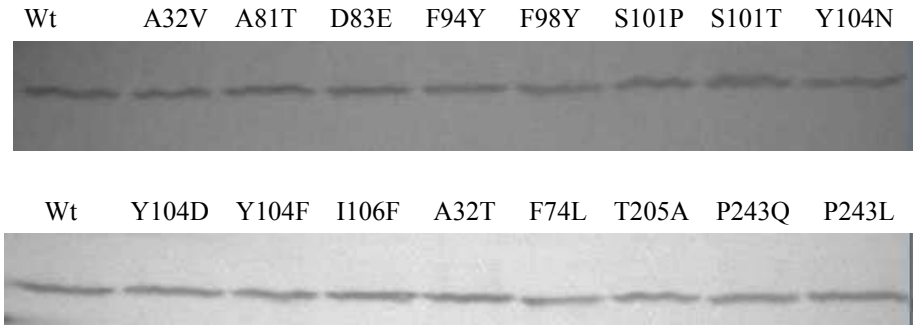

Figure 2.3. Western blots demonstrating the stability and relative quantity of EsaR* variants containing the critical amino acids. The 28 kDa EsaR band was visualized with anti-EsaR antibody. The positive control is the wild-type EsaR induced by arabinose and each blot was performed in duplicate. The numbering above the western blot indicates the amino acid substitution in the EsaR* variants.

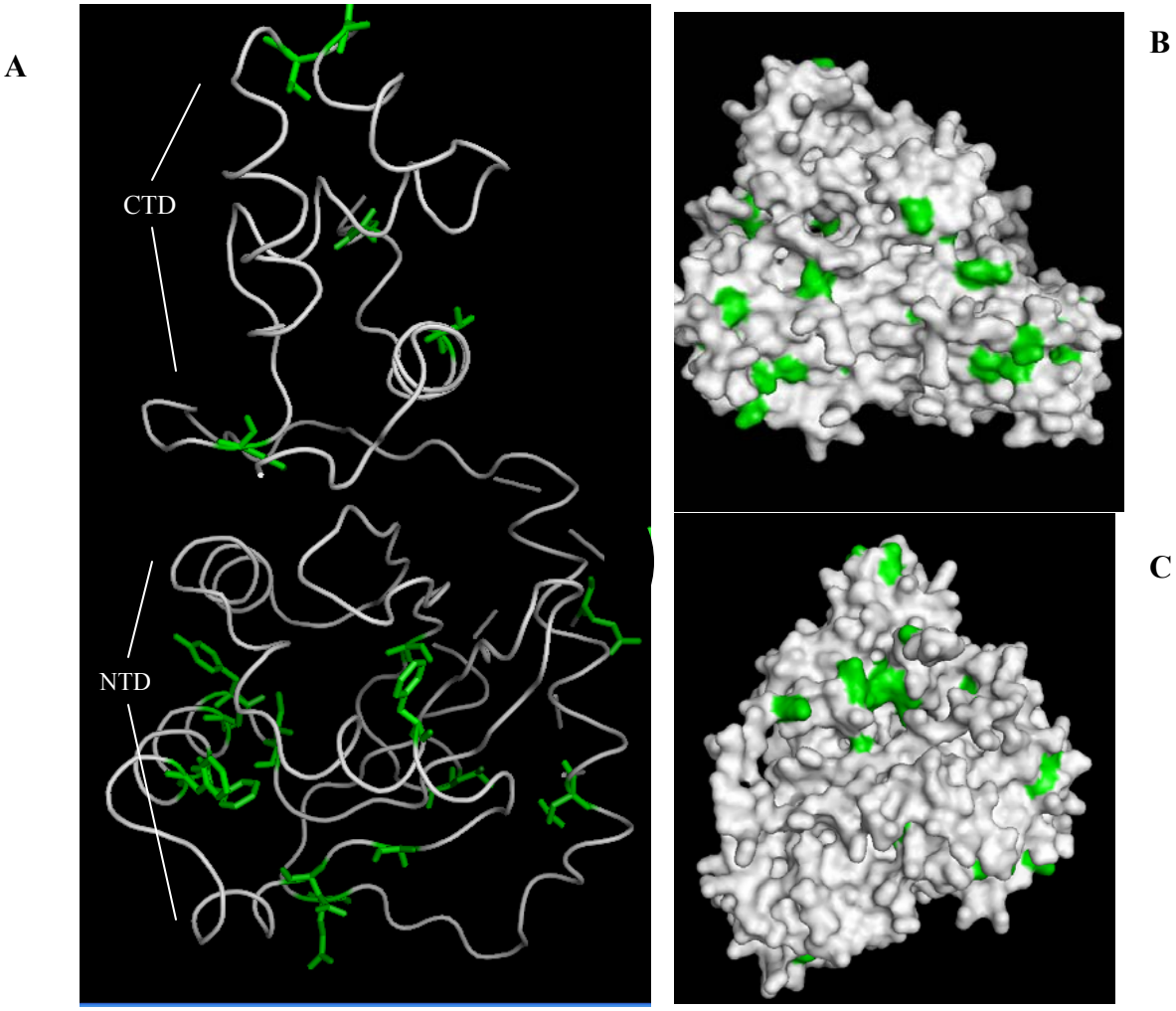

Figure 2.4. Placement of all amino acid substitutions onto the homology model of EsaR. All amino acid substitutions discovered via error-prone PCR and screening were mapped using the program PyMOL, on a homology model of EsaR. This model is based on the crystal structure of TraR (Zhang et al, 2002). The amino acid substitutions mapped, and colored in green, are those labeled as such in Table 2.8. A. A cartoon depiction of EsaR with the positions of all substitutions shown. B. A surface depiction in the same orientation as (A) of EsaR which show the amino acids exposed to the extracellular medium. C. An illustration of EsaR with amino acid substitutions in a 180º rotation from (B).

domain may effect the release of the DNA. Beyond directly impacting AHL binding, C-terminal variants that bind to the DNA with a greater affinity would also be acquired through the screening process.

In order to assess these theories, variant strains containing multiple mutations were dissected apart and tested individually through the repression assays. This helpd determine which mutations caused a loss of responsiveness to AHL versus those that occur by coincidence. Of the 25 distinct amino acid substitutions, 5 were found to be single AA substitutions achieved through error-prone PCR. This left 20 AA that needed to be separated via site-directed mutagenesis. Within these 20 mutations, multiple mutations were found within the same codon, resulting in different amino acid substitutions. By testing the affinity of the AHL for a variety of amino acids within the same mutated codon, properties about the bonding interaction between a critical AA and AHL may be inferred.

The quantitative β-galactosidase assays of the variants derived through site-directed mutagenesis and error-prone PCR showed that 11 mutations at nucleotides 95, 241, 249, 281, 296, 301, 302, 310A, 310G, 311, and 316 encoding for 8 amino acid substitutions at residues 32, 81, 83, 94, 98, 101, 104, and 106, exhibit the EsaR* phenotype (Figure 2.5). This assay also indicated that there are mutations at five nucleotides 94, 220, 613, 728A, and 728T, which amount to three additional amino acid substitutions at residues: 74, 205 and 243 exhibiting a phenotype intermediate between the wild type and other EsaR* variants. Residue 32 was previously found to be a noninducible repressor at the mutated nucleotide 95, as well as an intermediary repressor at mutated nucleotide 94. Relating these critical and intermediary substitutions to their

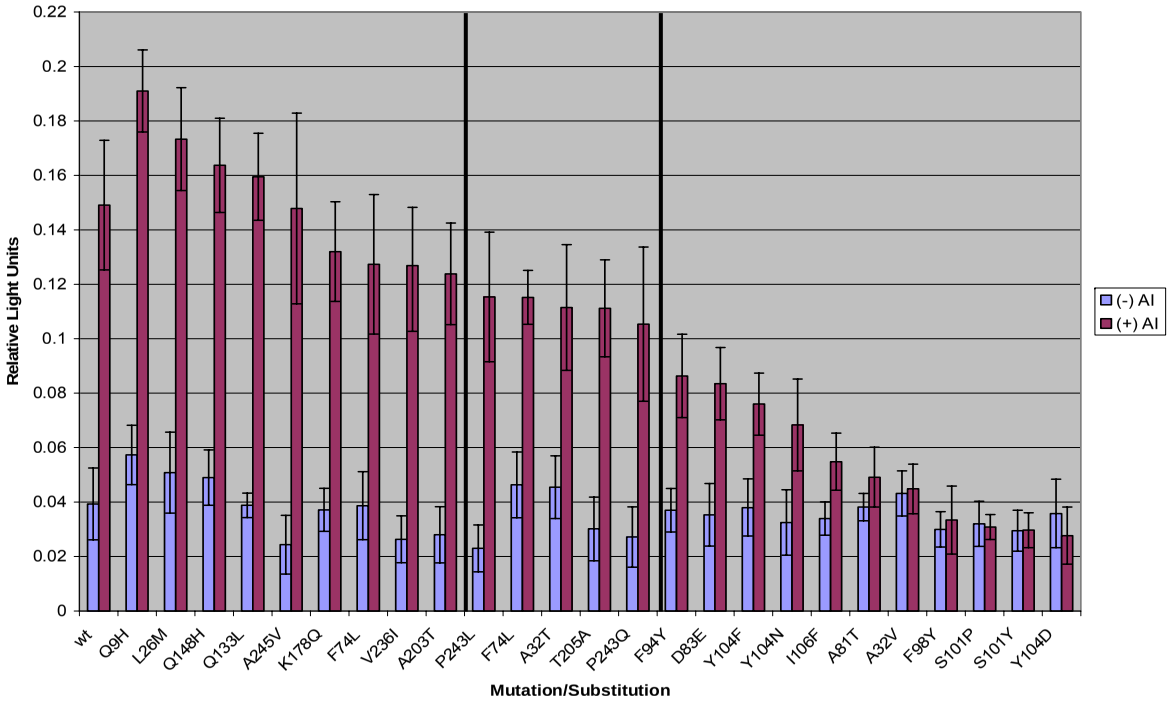

Figure 2.5. β-galactosidase assays of all EsaR* variants generated by site-directed mutagenesis. Two independent samples which contained the variant *esaR* constructs cloned into pBAD22 were assayed in triplicate for LacZ activity as described in the text in the presence and absence of AHL. Substitutions A32V, A81T, D83E, F94Y, F98Y, S101P, S101T, Y104N, Y104D, Y104F and I106F result in noninducible repressor activity of EsaR* variants, while substitutions A32T, F74L, T205A, P243Q, and P243L encoded EsaR* variants with intermediate activity.

amino acid properties 9 residue substitutions contain biochemical changes at the following residues: A32T, A81T, F94Y, F98Y, S101P, Y104D, Y104F, T205A, and P243Q.

It is interesting to note that four amino acids, 32, 101, 104, and 243 were altered multiple times, resulting in different amino acid substitutions that cause varying degrees of repression. The remaining substitutions, A32V, F74L, D83E, S101Y, Y104N, I106F and P243L produce static amino acid substitutions in terms of their chemical properties. Residue 32 is changed by base pairs 94 (A32T) and 95 (A32V), where nucleotide 95 is a greater non-inducible repressorin the presence of AHL. The substituted valine may cause EsaR to become locked in a conformational change that prevents it from responding to the AHL. Valine contains a bulkier side chain than threonine or alanine and may potentially alter the flexibility of the protein, not allowing it to interact with the AHL. The amino acid substitutions at 104 are due to changes at nucleotides 310A (Y104N), 310G (Y104D), and 311 (Y104F) respectively. The variant translated from template with mutated nucleotide 310G (Y104D) represses *lacZ* to the greatest degree. Tyrosine may be donating hydrogens to the AHL or other surrounding amino acids forming hydrogen bonds. When it is substituted with amino acids that change polarity, as in phenylalanine, or charge as in asparagine, the hydrogen bond can no longer be formed with the AHL or surrounding amino acids. Perhaps the substituted residues form a weaker van der Waals bond, and the stability of the EsaR-AHL complex becomes compromised. Another interesting residue identified through mutagenesis is amino acid 101, encoded by the mutated gene at base pair 302 (S101Y). The serine is substituted with threonine, whose side chain is of a similar size to that of serine. Although there is a small structural

change, there is a large effect on the degree of repression in the presence of AHL. This may indicate that this residue is specific for the AHL-EsaR interaction by directly interacting with the AHL, perhaps by a hydrogen bond due to the hydroxyl group within the side chain. Lastly amino acid 243 was changed by two different mutations at nucleotide 728A (P243Q) and 728T (P243L). The variant with this substitution is considered to have an intermediary effect on AHL binding. Therefore the substitution will likely alter EsaR so that it may have a better binding affinity for DNA. Residue 243 is part of the codon for proline, which breaks off the alpha helix in proteins. As proline has been substituted with other residues (see Table 2.3), the alpha helix may be elongated and provide a greater interface for the EsaR-DNA interaction, enabling a more stable complex. As these two mutations produce variants that effect derepression relatively equally, no pattern can be established as a result of amino acid differences.

The variants with intermediate activity have amino acid substitutions that are mostly located within the C-terminal domain. This may indicate that these substitutions alter the structure of EsaR by creating a rigid protein that is unable to interact with AHL, as described above. Additionally, these substitutions may allow a greater affinity of EsaR for the DNA, causing derepression less likely to occur.

Interpreting the crystal structure data

Although numerous amino acids substitutions have been generated through this mutational study, only a vague hypothesis can be formed in regards to locating a potential binding pocket located within EsaR. Of the listed amino acids (Table 2.3), four have been identified to be involved in AHL binding within LasR and TraR, and include EsaR residues 32, 98, 101, and 106 (Figure 2.6). All four amino acids are engaged in van der

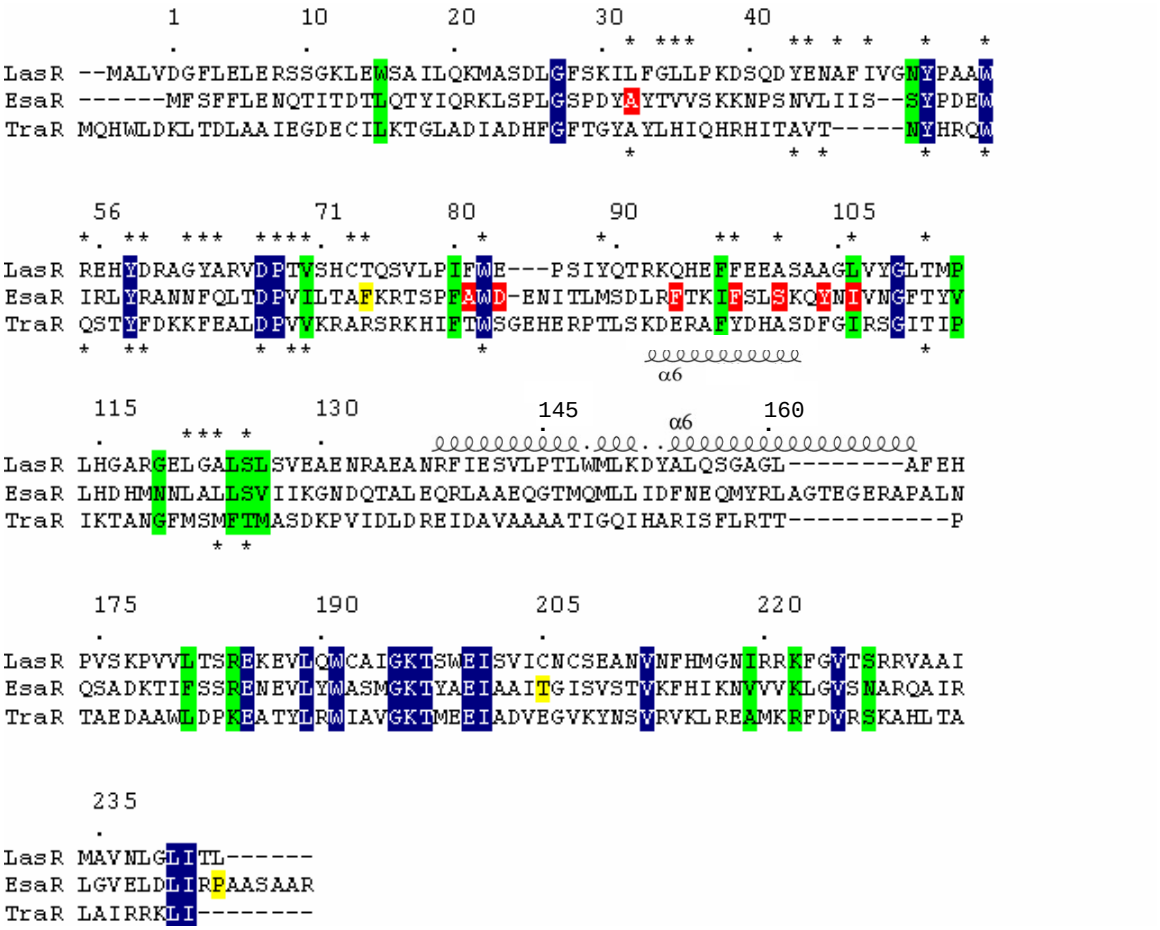

Figure 2.6. A clustal alignment of LasR, EsaR, and TraR. Sequences were aligned using Biology Workbench, with modifications as appropriate according to literature (Stevens and Greenberg, 1999; Bottomley et al, 2007). Asterisks indicate residues involved in the AHL binding pocket of LasR (above) and TraR (below). The red residues are critical for the EsaR* phenotype; yellow residues are substitutions resulting in intermediary repression; green indicates conserved, functionally similar residues; blue shading indicates invariant residues. Residues important for dimerization are indicated by the α6 helices located for LasR (above) and TraR (below). Numbering is for EsaR.

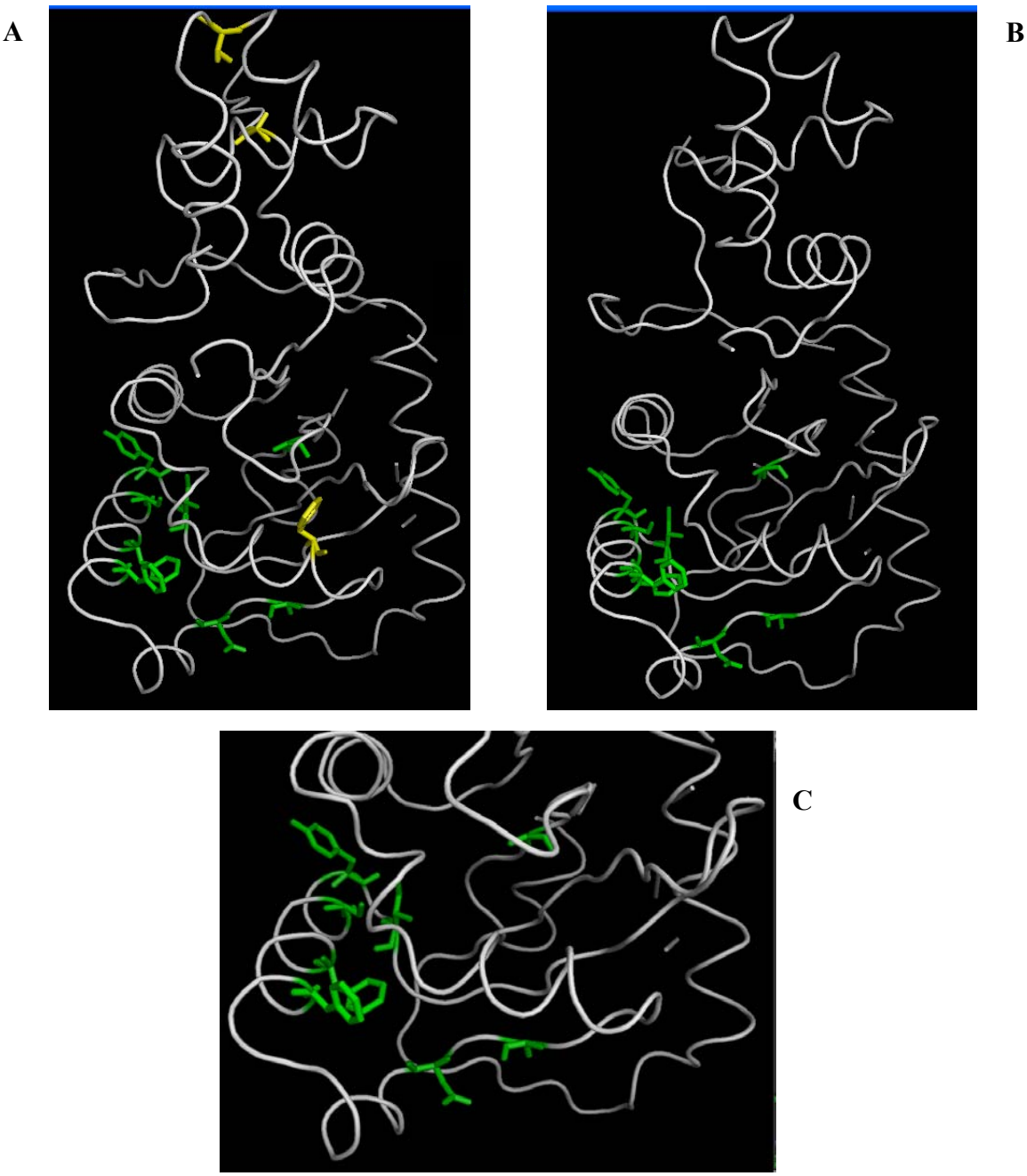

Figure 2.7. The location of the critical and intermediate residues mapped within the homology model of EsaR. A. Using PyMOL, the side chains of the critical amino acids, 32, 81, 83, 94, 98, 101, 104, and 106, are exposed and colored in green, showing a potential binding pocket within the protein. The intermediary residues, 243, 205, and 74, are shown in yellow, and map some distance away from this pocket. These may effect the conformation of the protein or the DNA-EsaR* interaction. B. A picture of the EsaR homology model without the intermediary residues highlighted. C. A close-up view of the potential binding pocket within EsaR for the AHL.

Waals interactions between AHL and TraR (Zhang et al, 2002). In addition, it has been shown that these residues form the ligand binding pocket of LasR (Bottomley et al, 2007). Mapping these amino acids, in conjunction with the remaining critical residues, onto the homology model of EsaR reveals a heavily mutated region within the N-terminal domain (Figure 2.7). Similarly, the mapping of the corresponding amino acids onto TraR and LasR show a comparable mutated region in the LasR, TraR, and EsaR. Amino acids 32, 81, and 83 are positioned slightly differently in the N-terminal domain, while amino acids 94-106 are similar in location on the structure of LasR (Figure 2.8). These disparities may be due to the long acyl chain of the cognate AHL of LasR as compared to TraR and EsaR; the longer chain may require the internal structure to be rearranged for its accommodation.

Two valid conclusions can be made from the structural mapping observations of the N-terminal domain. The first of which is that EsaR, TraR, and LasR have similar, but not identical, structural configurations. The AHL is imbedded in the hydrophobic regions of the protein. This would mean that altering residues 32, 98, 104, and 106 within EsaR, shown to be important in TraR and LasR, cause conformational changes within the N-terminal region such that the AHL cannot make a stable interaction. The substitution may also refold the protein in such a way that these critical amino acids are not readily available to the AHL.

The second conclusion, is that the predicted structure of EsaR is unique among the structures of LuxR-type activators identified thus far. Amino acids 32, 81, 83, 94, 98, 101, 104, and 106 may all be directly involved in AHL binding, and located within a different region in EsaR as compared to TraR. Support for this hypothesis can be found

A B

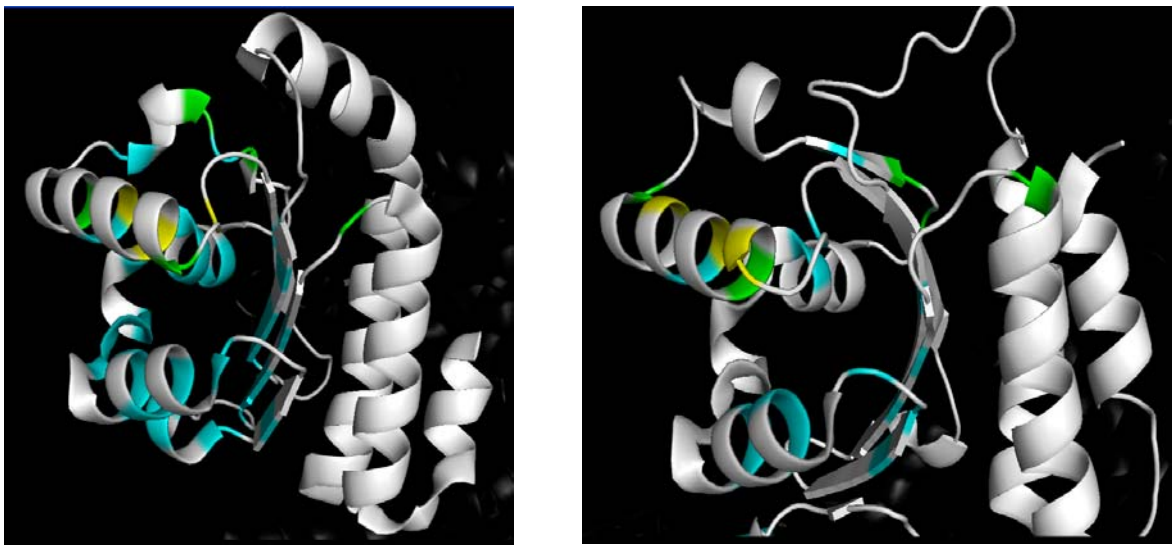

Figure 2.8. Amino acid substitutions of EsaR* variants mapped on LasR and TraR. Using PyMOL, the eight critical amino acid substitutions, 32, 81, 83, 94, 98, 101, 104, and 106, have been mapped onto LasR (Protein Data Bank code 2UV0) shown) and TraR (Protein Data Bank code 1L3L). (A) The crystal structure of LasR is colored in white. Residues of LasR involved in AHL binding are colored in cyan, the critical residues of EsaR are green, and those residues which are shared between LasR and EsaR are in yellow. (B.) The crystal structure of N-terminal region of TraR, in white. The color scheme of the residues of TraR are identical to that of panel A.

in a comparison of the known crystal structures of LasR and TraR. Differences between the acyl chains cause spatially conserved residues to exhibit different functionalities in the presence of AHL, as a result of the AHLs flexibility (Bottomley et al, 2007). These changes cause the AHL binding pocket to consist of different critical residues between LasR and TraR. From this, Bottomley et al concluded that these differences within the binding pocket make a LasR homology model based on TraR inappropriate. This same principal may be applied to the homology model of EsaR, based on TraR, as the acyl chain differs by two carbons. This creates the possibility of a different location for the AHL binding pocket within EsaR. The location of this potential binding pocket may be shallow and near the surface of the protein, consisting of the critical amino acid substitutions identified in this study. It is important to note that the 2-carbon structural difference between the AHLs of EsaR and TraR may indicate that the EsaR homology model is not entirely accurate, with an erroneous placement of the AHL binding region. The critical amino acids found experimentally, independent of the model, suggest that the binding pocket of EsaR is closer to the surface of the protein due to the number of substituted, polar amino acid residues. Further work in generating substitutions either independently of the model through error-prone PCR or dependently through site-directed mutagenesis according to the alignment of LasR and TraR (Figure 2.6) is necessary to pinpoint an AHL binding pocket.

Relating the results to published literature

Further support for an AHL binding region different from that of TraR or LasR can be found within the paper published by Minogue et al in 2002. Two separate *in vivo* studies showed that as AHL is added exogenously to a growing culture, EsaR responds

rapidly by deprepression. This was demonstrated through β-galactosidase assays in constructs similar to reporter strains created in this study, as well as fluorescence quenching experiments that show EsaR interacts specifically and stoichiometrically with the AHL. Surface plasmon resonance also revealed that as the concentration of AHL increases, the amount of EsaR capable of forming a complex to the DNA decreases. Together, these experiments show that the AHL binding region must be located close to the surface of EsaR enabling a reversible reaction. It is unlikely for AHL to become imbedded within the protein post-translationally, as is required in TraR and LasR. This surface-exposed pocket is given further support by the number of critical polar residues identified in this study.

Consequently, *in vitro* assays demonstrate the opposite effect. Within mobility shift assays (EMSA), the AHL does not promote dissociation of the EsaR-DNA complex when added exogenously. Instead, EsaR remains bound. This experiment could suggest that the binding pocket for the AHL within EsaR is imbedded in a hydrophobic portion of the protein. However, strong evidence suggests otherwise: AHL binding is reversible within *in vivo* assays (Minogue et al, 2002). It was shown that the EsaR homologue ExpR releases DNA during EMSA in the presence of AHL (Reverchon et al, 1998). Finally, several critical surface residues were identified in this study. Therefore, all of the results this suggest that the AHL binding pocket within EsaR is not similar to TraR or LasR, but perhaps is closer to the surface of the protein.

Effects of a mixed EsaR-EsaR* population of DNA binding

Since the mutagenized *esaR* is present on a higher copy number plasmid in comparison to the wild type, the ratio of variant homodimers will be greater as compared

to wild type homodimers or heterodimers. It is not surprising then, that the degree of repression of the *lacZ* gene in the presence of AHL is similar to that of the positive control in the absence of the AHL (Figure 2.9), although these results are preliminary. As the level of LacZ activity is consistent among a majority of the variant strains, it suggests that the variant phenotype is dominant over the wild type. It also implies that the heterodimers formed are still capable of binding to the DNA in the presence of the AHL, despite the wild type half of the dimer being presumably no longer bound. There may be a high degree of affinity of the variant for the DNA, compensating for the instability of the heterodimer in the presence of the AHL.

While most of the variants are dominant over the wild-type EsaR, there are two strains where there is elevated expression of *lacZ* in the presence of AHL, and include D83E and F94Y. Amino acid substitution D83E initially shows in Figure 2.5 that it does retain some degree of response to the AHL as it is in close proximity to the intermediary repressors. This degree of response is confirmed again in Figure 2.9 as β-galactosidase activity is elevated, but still less than half-fold that of the positive control. Because this activity is similar in separate studies (Figures 2.5; 2.9), the variant can be considered to be dominant over the wild type. Why F94Y responds at a level two-fold higher than the positive control in the presence of the AHL is unknown.

Purification of EsaR

Distinguishing the amino acids most directly involved in binding AHL requires a determination of the affinity of the AHL for EsaR* in comparison to the wild type.

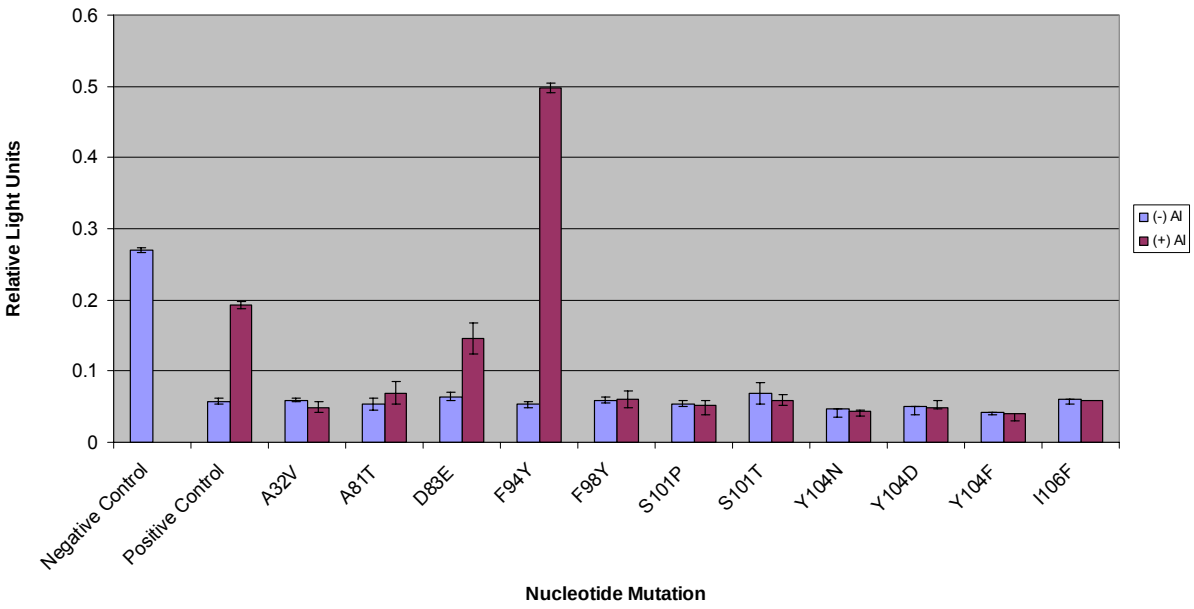

Figure 2.9. Preliminary β-galactosidase assays demonstrating whether the variant is dominant. B-galactosidase assays were performed in accordance with the text using pRNP-*lacZ*, pSUP102-*esaR*-wt, and pBAD22-*esaR**. The positive control contains pRNP-*lacZ*, pSUP102-*esaR*-wt, and empty vector pBAD22, while the negative control contains pRNP-*lacZ* and empty vectors pSUP102 and pBAD22. The variant protein appears to be dominant over the wild-type EsaR. Samples were tested in one experiment in triplicate.

Hence, protein melting assays and fluorescence spectroscopy were utilized to examine the AHL-EsaR interactions. As has been previously described, the AHL causes EsaR to become more thermally stable in its presence and provides a method for determining the EsaR*-AHL affinity – the degree of stability of EsaR* in the presence of AHL. However, in order to assess this attraction a baseline must first be established with wild-type EsaR. Purification of full-length EsaR is possible, but can be achieved only through a laborious protocol (Minogue, 2002). Efforts to improve the speed and efficiency of purification have resulted in the use of a His-MBP tag (D. Schu, unpublished results). This tag consists of six His residues, the maltose binding protein (MBP) amino acids, a sequence cleavable by TEV protease and six glycine residues. The His-MBP residues are a necessary component as they aid in the purification and solubility of the protein. The TEV protease sequence was subsequently added to allow cleavage of the His-MBP sequence from EsaR, resulting in a pure form of EsaR. However, it was found that cleavage of the tag was inefficient, and mixed heterodimers formed within the column preventing the purification of a tagless EsaR. The glycines were then added to the sequence so that the tag would be separated from the protein in a failed attempt to improve the cleavage efficiency.

Establishing a baseline of affinity of EsaR for AHL

Although purification is achieved and the functionality of EsaR is maintained with regard to AHL and DNA binding (D. Schu, unpublished results), the presence of the bulky tag may prevent the interaction between the AHL and EsaR from being detected. This was shown within the protein melting assays. In this assay as the RT-PCR thermocycler heats to higher temperatures, the domains should unfold in the order of

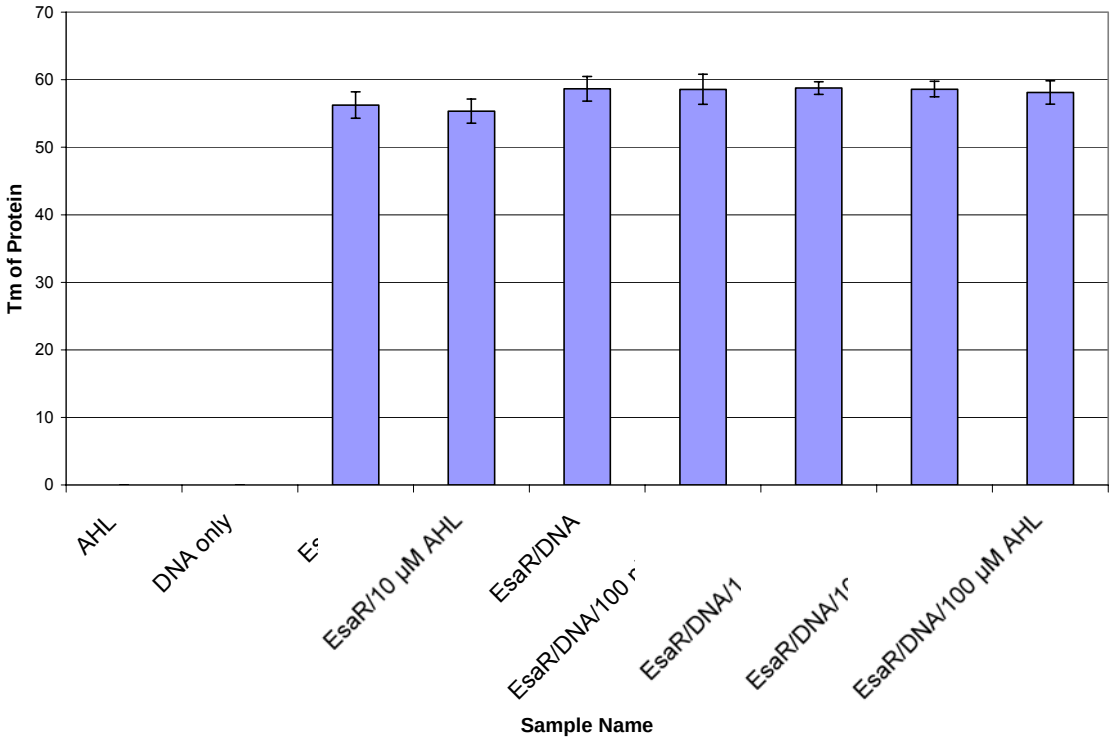

Figure 2.10. The thermal stability of EsaR in the presence and absence of AHL. His-MBP-EsasR was exposed to the DNA as well as increasing concentrations of AHL as the RT-PCR increased the temperature over time. Each sample was tested in triplicate. As can be seen, the stability of EsaR remains constant, and is not effected despite a 100-fold excess of AHL as compared to EsaR at a concentration of 1 mg/ml, though it binds in a 1:1 ratio.

C- terminal, N-terminal, and protein tag (F. Schubot, personal communication). By adding DNA to the mixture the C-terminal region becomes stabilized allowing for the dissociation of the N-terminal region to be measured properly. DNA containing the *esa* box was added to each experimental set while the concentration of AHL was varied, in order to establish a concentration in which EsaR responds to the AHL. Despite the variation of AHL even in

100-fold excess, the stability of EsaR remained constant (Figure 2.9). This may be due to the N-terminal domain tag that is 20 KDa larger than EsaR. The tags sheer bulk may be preventing any unfolding of EsaR from being observed, masking its effect. Additionally, the tag is highly thermally stable. Therefore, the RT-PCR thermocycler may be detecting the unfolding of the tag as opposed to EsaR.

Since this approach was shown to be unsuccessful a different technique, fluorescence spectroscopy, was employed. As Minogue et al, 2002 have established, EsaR contains an inherent fluorescence, which is quenched upon binding to the AHL. By comparing the amount of quenching of the AHL-EsaR* complex as compared to the wild type, the importance of the amino acid residue for the AHL-EsaR interaction can be determined. Using a RF-1501 spectrofluorophotometer the excitation wavelength of EsaR was determined to be 281 nm, while the emission was 339 nm. However, when the protein was subjected to the UV light for fluorescence measurement, it was found that the fluorescence intensity units (FI) decreased rapidly over time in the absence of AHL. This may indicate that EsaR is degrading under UV light by photooxidation. The UV light may cause tryptophan to degrade into a series of oxygens, thus breaking down the protein (Robert White, personal communication). Attempts at measuring the fluorescence

intensity of BSA as well as tryptophan itself yielded the same degradation of the signal, while the fluorescence of small molecules appeared to stabilize after a small decrease. Therefore, determining whether quenching is occurring is nearly impossible as it is uncertain whether the decrease in fluorescence is due to the binding of the AHL or protein degradation.

Since the FI decreased over time not only with EsaR but with the control protein and tryptophan, it may be possible that this particular instrument is not functioning properly. Therefore, the use of another instrument was necessary. A 96-well plate reader, SPECTRAfluoro Plus (Tecan, Switzerland), has the ability to be read the fluorescence intensity of various compounds. As the excitation wavelength and emission wavelength have been previously determined, these values were transferred to the plate reader and a stable fluorescence of EsaR was observed (Figure 2.11). However, upon the addition of the AHL, only an approximate 7% decrease in the fluorescence was observed when the AHL was added in 10-fold excess. These results may be due to the large, highly fluorescent tag, which may mask any large degree of quenching. A greater degree of quenching using 100-fold or more excess of AHL has yet to be experimentally tested.

Yet another way to determine the affinity of AHL for EsaR is through indirect protease studies. EsaR, with the protein tag, has been shown to be differentially digested by proteases in the presence and absence of AHL (D. Schu, unpublished results). This suggests that there are conformational changes occurring within EsaR upon interacting with AHL. Therefore, not only will this biochemical test determine how well the AHL interacts with EsaR* through the digested band strength, but any conformational changes

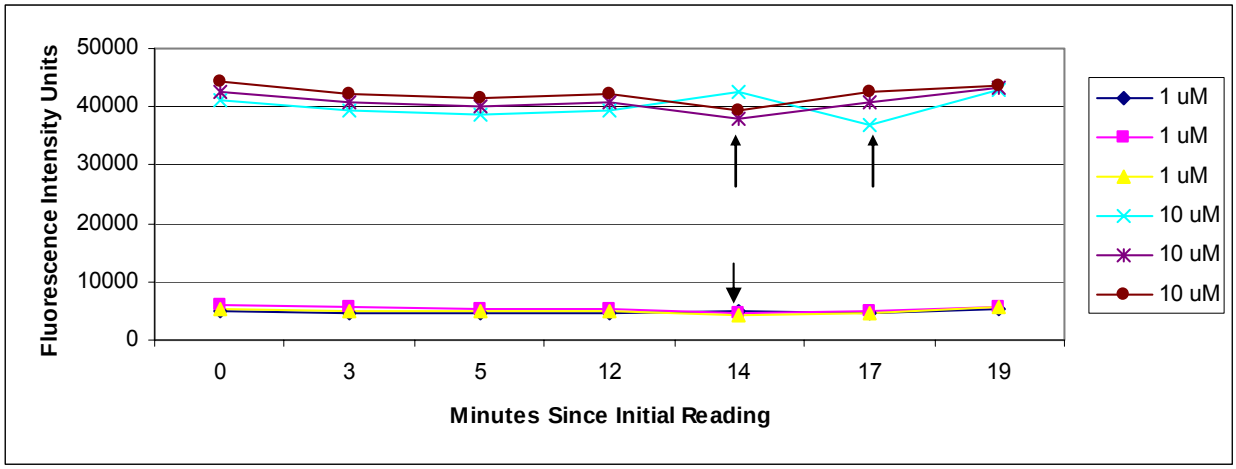

Figure 2.11. Determining fluorescence quenching through the 96-well plate reader. Two different concentrations of His-MBP-EsaR were subjected to equivalent and excess concentrations of AHL. The 1 μM protein concentration was exposed to equivalent AHL, while the 10 μM concentration was exposed in 10-fold excess. The arrows indicate the time point when AHL was added to the well.

within the variant may be seen as well.

It is also possible to determine how the amino acid substitution affects the affinity of the variant for the DNA. Electromobility shift assays can be used to generate a titration curve and subsequently establish a dissociation constant for the variant. By comparing these constants to wild-type EsaR, differences in variant affinity for the DNA can be determined.

Concluding remarks

This study has identified several unique amino acids within EsaR that effect the AHL-EsaR interaction not found within TraR or LasR. Specifically, these residue substitutions allow EsaR to retain its repressor activity despite the presence of AHL. Whether or not the mutations in *esaR* leading to the EsaR* variants are genetically dominant still remains to be determined. In addition, by further studying the effect of these substitutions on the affinity of the AHL for EsaR, and also for the DNA, a potential binding pocket and derepression mechanism may be elucidated.

Chapter III

Determining the Stability of the N-Terminal Domain and the Dimerization Region of EsaR

Introduction

It is known through electrophoretic mobility shift assays that EsaR exists as a dimer in the absence of AHL, and can bind to the DNA (Minogue et al, 2002; von Bodman et al, 2008). However, the location of this dimerization region in the peptide sequence has yet to be elucidated. This study aims to isolate a potential region of dimerization within EsaR by examining the ability of the protein to dimerize in the presence of AHL, after truncations were made within the C-terminal domain (CTD). Truncations of EsaR have been generated, both leaving and including the extended interdomain linker region with the N-terminal domain (NTD) at residues 178 and 169 respectively. Constructs for a dominance assay were then created in which the wild-type *esaR* and the truncated *esaR* were transformed into the same cell on separate plasmids. A third plasmid is also present within this strain that encodes a reporter capable of being repressed by dimeric forms of the regulatory protein.

Genetic dominance assays were used to determine if the truncated protein was able to dimerize with the wild-type EsaR, resulting in the formation of heterodimers capable of repressing the *lacZ* reporter. Preliminary results suggest that the dimerization region of EsaR is within amino acids 1-160 (D. Schu, unpublished results). While the data presented here does not reflect this recent finding, the methods and data analysis of this study can still be employed for further investigations into pinpointing the exact region of dimerization. These efforts have proven that the NTD of EsaR is stable in the absence of the C-terminal domain. This may help facilitate future efforts to analyze the NTD structure via NMR.

Methods and Materials

A. Strains, plasmids, and growth conditions

All experiments were performed in either *Escherichia coli* Top10 or DH5α. The reporter plasmid used in each study described below contained the *esa* box::*lacZ* within pEXT22 and is referred to as pRNP-*lacZ* (Table 3.1). Wild-type and truncated forms of *esaR* are under the control of the P_{tac} promoter, and were induced with 500 μM IPTG. Ten μM AHL (3-oxo-L-C6-homoserine lactone), diluted in 100 μl of ethyl acetate, was added to the test tubes and allowed to evaporate prior to culturing for dominance assays. Strains for the dominance assays were first grown in LB medium and subsequently subcultured into RM minimal medium (2% casamino acids, 1x M9 salts (From 10x stock: 128 g/L Na_2HPO_4, 30 g/L KH_2PO_4, 5 g/L NaCl, 10 g/L NH_4Cl), 0.4% glucose, and 0.1 M $MgCl_2$ containing 100 μg/ml ampicillin (Ap100), 50 μg/ml kanamycin (Kan50), and 20 μg/ml chloramphenicol (Cm20).

B. Creating N-terminal domain truncations

Two primers were created (HIN169 and HIN178) (Table 3.2), which bind to a region of *esaR* at the 3' end of the region encoding the N-terminal domain or the N-terminal domain plus the linker region respectively. A third primer, NSMAES (Table 3.2) was used to bind to the 5' start site of the *esaR* gene and amplify from the N-terminal region inward towards the internal region of the gene. Two different reactions were assembled containing either NSMAES and HIN169 or HIN178 as follows: 1x Thermo Poly Buffer, 200 μM of each dNTP, 1 U of Deep Vent Polymerase (New England Biolabs (NEB), Ipswich, MA), 100 ng/μl of the template (pBAD22-*esaR*), 500 nM of each respective primer, and water to bring the reaction volume to 50 μl. The

thermocycler was programmed as follows: 1 cycle: 95°C for 2 minutes; 30 cycles: 95°C for 30 seconds, 58°C for 1 minute, 75°C for 1 minute; 1 cycle: 75°C for 10 minutes. The reactions were electrophoresed on a 0.8% agarose gel and the appropriate fragments were purified using Qiaquick Gel Extraction Kit as suggested by the manufacturer (Qiagen, Valencia, CA).

dATPs were added to the ends of the isolated fragment to create a poly A tail under the following conditions: 1x Thermo Poly Buffer, 200 μM dATP, and 1 U of *Taq* Polymerase (NEB). This reaction was carried out for 20 minutes at 72°C. This generated sticky ends onto the fragment and facilitated the ligation of the PCR product into pGEM-T (Promega, Madison, WI) (Table 3.1), after purification using the PCR purification kit (Qiagen). Following transformation of the ligation reaction into DH5α, blue/white screening ensued in order to confirm the proper insertion of the fragment. Cloning into pGEM-T causes disruption of the *lacZ* gene, and therefore white colonies were selected and are expected to contain the inserted fragment. After isolation of plasmids from the white transformants, samples were sent to the Core Sequencing Facility at Virginia Bioinformatics Institute (CSF-VBI) for sequencing. Once the nucleotide sequences were verified, a sequential digestion was performed using the enzymes *Sma*I and *Hind*III to cut the truncated fragment out and ligate it into a second vector, pKK223-3 (Brosius and Holy, 1984) (Table 3.2). The vector and fragments were digested with *Sma*I for approximately 2 hours at 25°C, after which, *Hind*III was added and allowed to digest for 2 hours at 37°C. The DNA was electrophoresed on a 0.8% gel and two bands of approximately 550 bp were purified from the gel. These fragments were then ligated into

Table 3.1. Strains and plasmids used in this study

Strain or Plasmid	Relevant Information	References
Strains:		
E. coli		
DH5α	F-Ø 80d*lacZ*ΔM15 Δ(*lacZYA-argF*) *U169 decR recA1 endAI hsd17 phoA supE44 thi-l gyrA96 relA1*	(Hanahan, 1983)
Top 10	F- *mcrA*Δ(*mrr-hsdRMS-mcrBC*) Ø 80d*lacZ*ΔM15 Δ*lac*X74 *deoR recAI araD139* Δ(*ara-leu*) *7697 galU galK rpsL* (Str^r) *endAI nupG*	(Grant et al, 1990)
Plasmids:		
pGEM-T	Cloning vector, f1 ori, Ap^r, used as an intermediate cloning vector	Promega
pEXT22	IPTG inducible vector, Kan^r	(Dykxhoorn et al, 1996)
pACT3	IPTG inducible vector, CM^r	(Dykxhoorn et al, 1996)
pACT3-*esaR*	*esaR* ligated into *Sma*I and *Hind*III sites in pACT3	This Study
pKK223-3	IPTG inducible vector, Amp^r	(Brosius and Holy, 1984)
pKK223-3-*esaR*	*esaR* ligated into *Sma*I and *Hind*III sites in pKK223-3	This Study
pHIN169	pKK223-3-*esaR* with deletion of residues 170-249	This Study
pHIN178	pKK223-3-*esaR* with deletion of residues 179-249	This Study
pRNP-*lacZ*	pEXT22 with the natural promoter region of *esaR* fused to *lacZ*	D. Schu, unpublished results

Table 3.2. Primers used in this study

Primer Name	Primer Sequence	Restriction Site
HIN169	5'AAGCTTTTACTAGGCTCGCTCGCCTTCGGTAC 3'	*Hind*III
HIN178	5' AAGCTTTTACTATTTGTCCGCGCTCTGATTTAAC 3'	*Hind*III
NSMAES	5' CCCGGGATGTTTTCTTTTTTCCTTGAAAATC 3'	*Sma*I

the *Sma*I-*Hind*III digested pKK223-3. The ligation reaction was transformed into DH5α. This vector will allow for the IPTG-inducible, overproduction of the truncated *esaR* gene. The truncation constructs within pKK223-3 are referred to as pHIN169 and pHIN178.

C. Performing a western blot

To check for the biological stability of the truncated EsaR variants, a western immunoblot was performed. *E. coli* Top10 strains containing either pKK223-3/*esaR*-wt, pHIN169, pHIN178, the empty vector pKK223-3, or no plasmids, were grown up from freezer stocks to an OD_{600} of 1.0 in 500 μM of IPTG to overexpress the truncated proteins and the wild type at 30°C. Aliquots of 1 ml were transferred to an eppendorf tube and the cells were pelleted through centrifugation. The supernatant was decanted, and the pellet was frozen at -70°C, which was subsequently allowed to thaw on the benchtop. The western blot procedure performed in this study is identical to that executed in Chapter II.

D. Constructing strains for the testing of dimerization

The wild-type *esaR* was moved from the high copy number vector pKK223-3 to the 11-copy number plasmid pACT3 (Dykxhoorn et al, 1996) (Table 3.2). A sequential digestion with *Sma*I and *Hind*III was performed as described above with both pKK223-3/wild-type *esaR* and pACT3. The pKK223-3/*esaR*-wt digestion produced an approximately 800 bp *esaR* fragment that was gel purified as suggested by the manufacturer (Qiagen) following electrophoresis. The purified fragment was then ligated to the digested pACT3 and the ligation reaction was transformed into *E. coli* DH5α. Of the resulting transformants, one colony was selected at random for plasmid purification. Strains with the desired combinations of plasmids were constructed via transformation as shown in Figure 3.1.

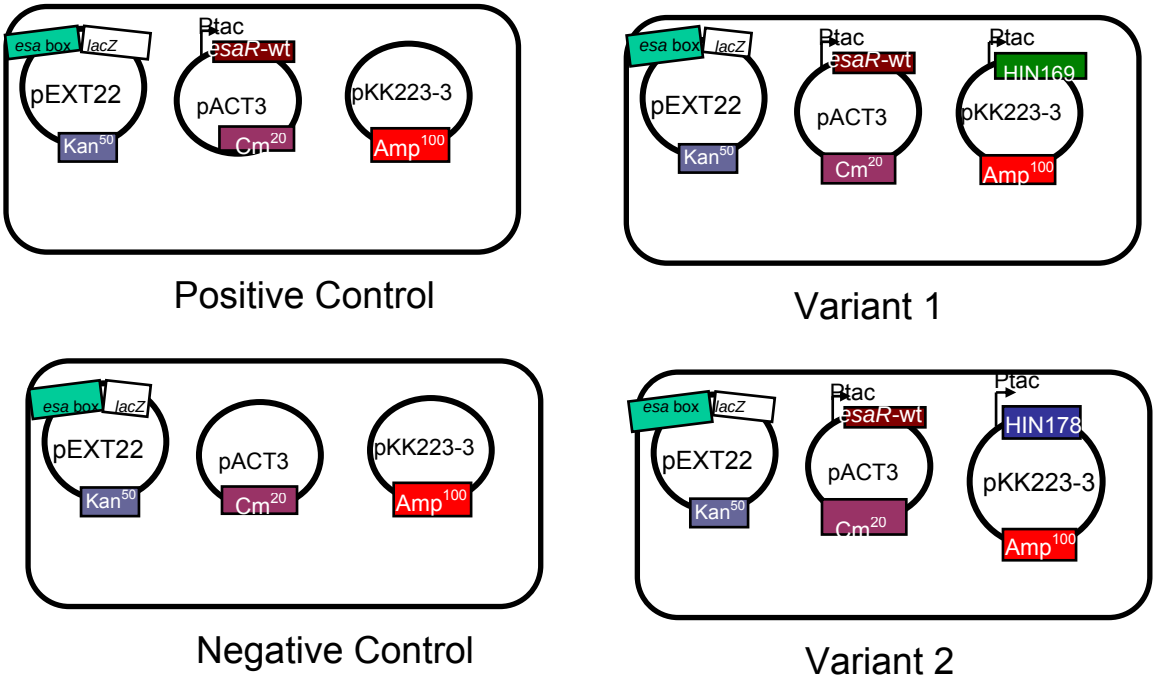

Figure 3.1. Strain construction for the dominance assays. Parent vector pEXT22 containing the *esa* box fused to the *lacZ* gene (pRNP-*lacZ*) served as the reporter plasmid in all strains. pACT3 contained the wild type *esaR*, while pKK223-3 encoded the truncated *esaR*.

E. Dominance assays

All four cell strains (Figure 3.1) were grown for approximately 7 hours from freezer stocks and subsequently subcultured into RM minimal medium. These cultures were grown over night at 30ºC. The following morning, the cultures were subcultured to an OD_{600} of 0.05 and induced with 50 μM of IPTG. The cells were grown to an OD_{600} of 0.5 at which point 5 μl aliquots were stored at -70°C freezer. β-galactosidase assays were then performed using a chemiluminescent reporter assay kit (Tropix, Bedford, MA) and a Beckman Coulter LD 400 microplate reader (Beckman Coulter, Fullerton, CA). The procedure was provided by the manufacturer.

Results and Discussion

The stability of the truncations

To better study the structure of EsaR, two C-terminal truncations were generated, designed to help identify the dimerization region of EsaR and analyze the stability of the NTD of EsaR. In addition to identifying the dimerization region of EsaR, these truncations may help to determine a mechanism by which derepression occurs. While it is hypothesized that EsaR is released from the DNA in the presence of acyl-HSL, other mechanisms for de-repression may be feasible. Perhaps EsaR is unable to maintain itself as a homodimer in the presence of the AHL.

Truncated EsaR variants were constructed through PCR amplification. The first truncation, referred to as pHIN169 (Table 3.1), contains the N-terminus only and the second variant, referred to as pHIN178 (Table 3.1), contains the N-terminus with the linker region. These truncations were then placed within an expression vector, for the overexpression of the truncated genes. Figure 3.2 demonstrates that the truncated forms of the *esaR* gene are biologically stable. However, the degree of stability does appear to vary a small amount between the pKK223-3/wild-type *esaR*, pHIN169, and pHIN178 constructs. The variant EsaR expressed from pHIN169 was produced at slightly lower levels as compared to the proteins encoded by pKK223-3/wild type or pHIN178.

Expected dominance assay results

Once the strains were constructed, dominance assays were subsequently performed to determine if the *esaR* variants are capable of dimerizing and binding to the *esa* box target within the cell. The truncated constructs within the pKK223-3 vector were transformed along with the wild-type *esaR* on a low-copy number plasmid into *E. coli*

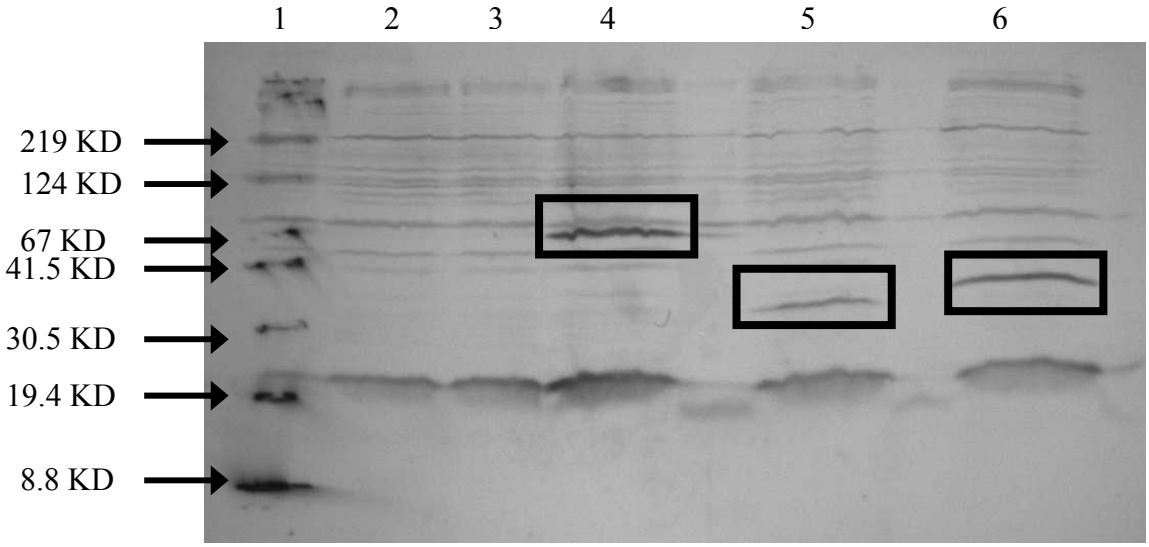

Figure 3.2. A western blot showing stability of the truncations. A western immunoblot containing truncated EsaR variants, negative controls, and a positive control. The boxes indicate where the biologically stable EsaR variants are located as well as the wild-type EsaR. Strains were induced with 1 mM IPTG and performed in duplicate (Lane 1-standard, 2- *E. coli* Top 10 only, 3- plus empty pKK223-3, 4- plus pKK223-3-*esaR*, 5- plus pHIN169, 6- plus pHIN178).

Top10 containing pRNP-*lacZ* (Table 3.1). The truncated fragments were present within a higher copy number plasmid in order to ensure detection of any phenotype due to their altered activity. β-galactosidase assays were used to indicate whether or not the truncated proteins are dimerizing.

A negative control strain contained the reporter plasmid and the two empty vectors pKK223-3 and pACT3. Expression of the *lacZ* gene was predicted to be relatively high as there is no EsaR present, in any form, to prevent its transcription. In contrast, the positive control strain contained the wild-type EsaR on pACT3, the empty vector pKK223-3, as well as the reporter plasmid. This combination should have caused repression of *lacZ*, with β-galactosidase activity levels to be approximately two-fold or lower in comparison to the negative control. It was initially hypothesized for the expression levels of pHIN169 to be lower than pHIN178, as the linker region was believed to be involved in dimerization. If this was true, pHIN169 would be deficient of the full proposed dimerization region. Subsequently, the variant would be unable to form a heterodimer with the wild-type EsaR. This would only allow for the wild-type EsaR homodimer to be functionally formed, repressing the *lacZ* gene similar to levels of the positive control. In contrast, if HIN178 contains the dimerization region, it would be able to compete for dimerization with the wild-type EsaR forming a heterodimer, as well as forming a truncated homodimer. As HIN178 lacks the C-terminal DNA binding domain it would be unable to bind to and repress the transcription of *lacZ* allowing for β-galactosidase levels comparable to the negative control. Complete activation may not be observed as there is still the potential for a wild type homodimer to form. A projected figure of the expected results can be viewed in Figure 3.3.

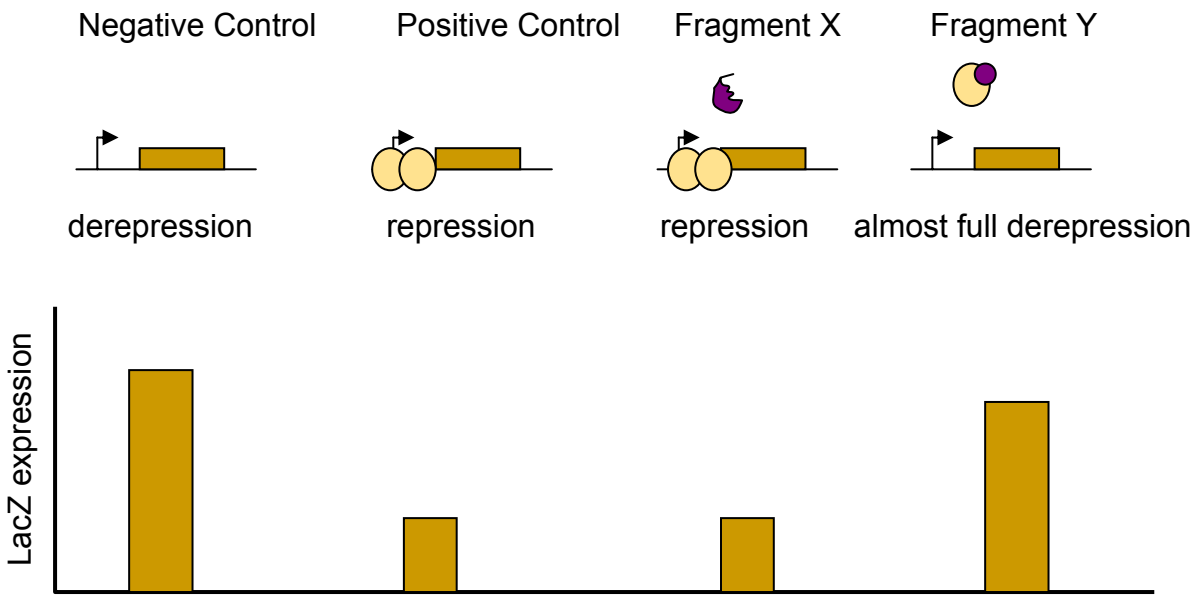

Figure 3.3. Proposed data for strains in the presence and absence of the dimerization region within the truncations. If the dimerization region was present within fragment Y, but absent in fragment X the following β-galactosidase activity pattern should emerge. Fragment Y is able to compete with and dimerize with the wild type. This causes less of the wild type to be available for forming a wild-type EsaR homodimer and there is less repression of the reporter strain. In contrast, if a region is proposed to lack this region, it cannot dimerize to the wild type and a wild-type EsaR homodimer is able to form, repressing the transcription of *lacZ* in levels similar to that of the positive control. These activation levels have been previously seen in dominance studies on LuxR (Choi and Greenberg, 1991).

However, if the dimerization region is within amino acids 1-160, as preliminary results suggest, the proposed activity levels of pHIN169 and pHIN178 outlined above will not be accurate. If both truncations contain the hypothesized dimerization region, the β-galactosidase activity levels of both pHIN169 and pHIN178 should have comparable levels of activation of *lacZ* with the positive control. Although each of the truncations are able to dimerize, they lack the C-terminal domain and therefore unable to bind to and repress the transcription of *lacZ*.

Observed results of the dominance assays

While the two truncations show similar results, they cannot be interpreted correctly as the positive and negative controls do not reflect what is expected in trials one and three (Figure 3.4A and Figure 3.4C). The positive control, which contains the wild-type EsaR and the reporter plasmid in the presence of the empty pKK223-3 vector, should be able to dimerize and fully repress the *lacZ* gene. In contrast, the negative control, containing all empty vectors with the exception of the reporter plasmid, contains lower activity as compared to the positive control. It was later discovered while attempting to make dominance strains for the dominant negative assays described in Chapter 2 that this strain did not produce a stable, wild-type EsaR in a western blot. More recently, the transformation of pACT3/wild-type *esaR* into *E. coli* Top10 already containing pRNP-*lacZ* yielded a high background of satellite colonies. As the *E. coli* strain contains a low level of resistance to chloramphenicol, the resistance marker of pACT3, it is possible that the randomly selected colony either does not contain the plasmid, or contains a variant form of the plasmid that may not contain *esaR* properly inserted into the vector. This would account for the similar levels of β-galactosidase

A

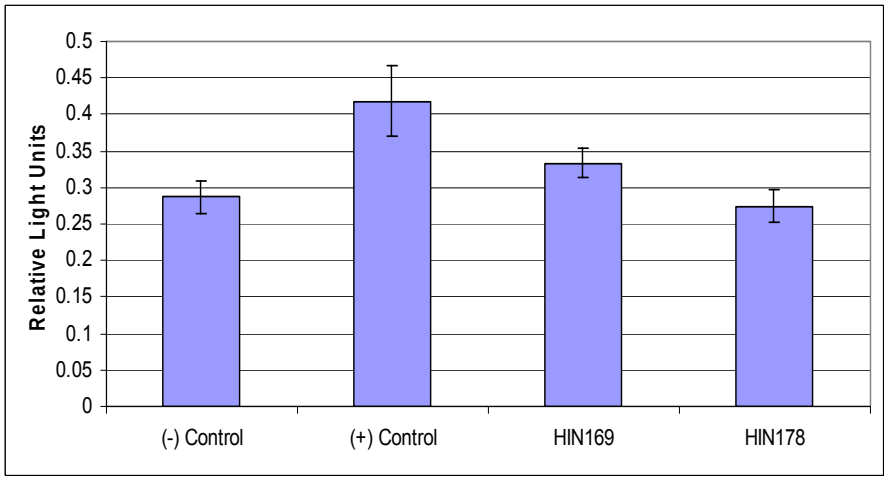

B

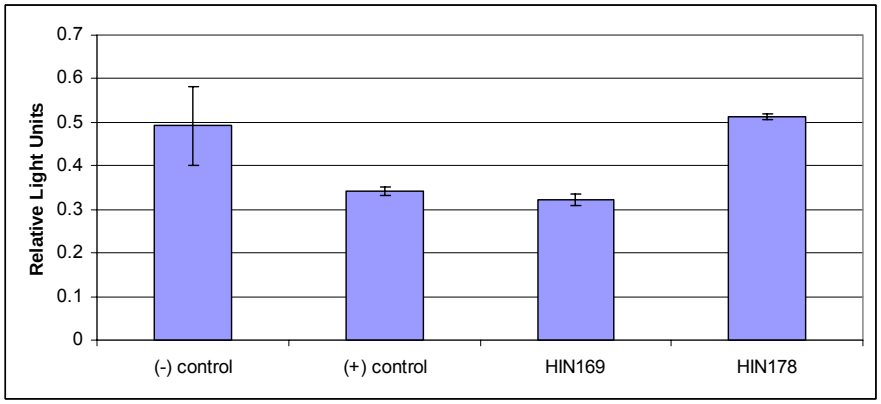

C

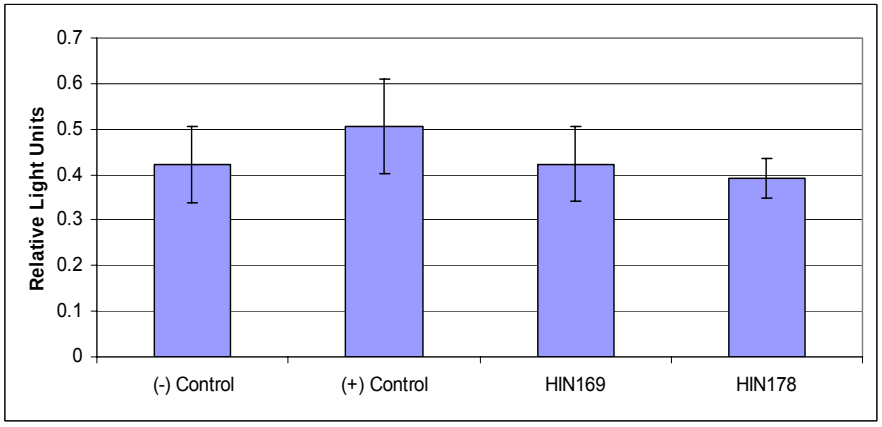

Figure 3.4. Dominance assay data as generated through β-galactosidase assays. (A.) The first trial of the dominance assay shows conflicting control results and therefore the experimental data cannot be verified. (B.) The second trial of the dominance assay contains control data similar to that which is hypothesized, however, the truncation data varies drastically. (C.) The third trial of the dominance assays again demonstrate conflicting control results, although the experimental data is shown to be similar as in trial one.

activity within the controls in trial three, after taking into account the standard deviation. Additionally, it is possible that the negative and positive controls were mislabeled when creating freezer stocks resulting in the contradictory results.

Despite the distrustful data seen in trials one and three as a result of the controls, trial two provided results that would be expected not only for the controls, but for a dimerization region present within HIN178 and absent from HIN169 (Figure 3.4B). It is currently unknown how these results were obtained as all three trials were identically performed and the data cannot be replicated (Figure 3.4C).

There are obvious flaws within the constructs seen in this portion of the study. To determine the reason for the varied data, a digestion using *Hind*III was performed. As there is one such restriction site in all three plasmids, it effectively tested for the presence of each of the three plasmids by linearizing the DNA and verifying the presence of the wild type and truncated insertions. While the appropriate reporter plasmid and various pKK223-3 plasmids were present in all strains, the plasmid pACT3-*esaR*-wt was absent from the variant strain containing the truncation HIN178 and missing the wild type gene in the remaining three strains (data not shown).

Future work on the dimerization region

A new plasmid containing the wild-type *esaR* has been constructed using the vector pSUP102 for the dominant negative assays in Chapter II. By moving the truncations onto the compatible pBAD22 and inducing with arabinose, data with the hypothesized results could possibly be achieved.

Determining the location of future truncations should rely on the crystal structures of TraR and LasR, LuxR-type proteins. Through these structures it has been shown that a

majority of the dimer-stabilizing residues occur within the α6 helices of TraR and LasR, which correspond to amino acids 132 through 161 of EsaR (Vannini et al, 2002; Bottomley et al, 2007). Three other conserved regions within LasR and TraR are involved in dimerization as well, and include α1, loop α4-β3, and loop β4-β5 (Bottomley et al, 2007). This corresponds to amino acids 3-10, 67-81, and 108-127 in EsaR respectively. As the α6 helix is considered to be the most important segment involved in dimerization, truncations or mutations within these additional segments may show only slight differences in the ability of EsaR to dimerize.

Chapter IV

Overall Conclusions

EsaR, a LuxR homologue in *Pantoea stewartii* subsp. *stewartii* utilizes an AHL-response mechanism opposite to that of the well-studied LuxR. At low cell densities, EsaR binds to and represses its target promoter. In a high cell population density the AHL binds to the transcriptional regulator EsaR and causes derepression. Where EsaR binds to AHL, in addition to its subsequent derepression mechanism is currently unknown.

A mutagenesis study was employed to identify amino acid residues involved in the AHL-EsaR interaction. Such mutants retained the repressor function despite the presence of the AHL. Eight amino acids were identified which caused EsaR* to become a constitutive repressor. Three additional amino acid residues provided EsaR* with intermediary repression in the presence of AHL; these residues were found to be primarily located within the C-terminus.

Plotting the location of the unique residues onto the 3-D structure of LasR and TraR, reveal that these substitutions occur in a region nearer to the extracellular surface than residues known to be involved in AHL binding in LasR and TraR. This may indicate that the binding pocket is differentially located in comparison to the homologous proteins. Strains containing these substituted residues may be further utilized in biochemical studies in an attempt to determine how specific residues are involved in interacting with AHL or effect the overall conformation of EsaR. Furthermore, strains containing the intermediary, C-terminal residue substitutions can be used to study the EsaR-DNA interaction.

Truncations were made at residues 169 and 178 and employed within a dominance assay in order to help elucidate a dimerization region within EsaR.

Unfortunately, these assays proved to be unsuccessful due to inappropriate positive and negative control β-galactosidase activity. Restriction mapping indicated that the vector containing the wild-type *esaR* has been incorrectly created and transformed. New constructs for the dominance assay are currently underway. However, western blot analysis did demonstrate that the N-terminal domain of EsaR is stable, which may help facilitate future efforts to elucidate its structure.

This study has identified several unique amino acid residues within EsaR that effect the AHL-EsaR interaction. These residues imply a novel binding pocket within EsaR. By utilizing these EsaR* strains in future biochemical studies, a potential binding region and derepression mechanism may be elucidated.

Chapter V

References

Atkinson S, Chang CY, Sockett RE, Cámara M, Williams P. (2006). Quorum sensing in *Yersinia enterocolitica* controls swimming and swarming motility. Journal of Bacteriolology 188: 1451-1461.

Bassler BL, Wright M, Silverman MR. (1994). Multiple signalling systems controlling expression of luminescence in *Vibrio harveyi*: sequence and function of genes encoding a second sensory pathway. Molecular Microbiology 13: 273-286.

Bassler BL. (1999). How bacteria talk to each other: regulation of gene expression by quorum sensing. Current Opinion in Microbiology 2: 582-587.

Bassler BL. (2002). Small talk: cell-to-cell communication in bacteria. Cell 109: 421-424.

Boettcher KJ, Ruby EG. (1990). Depressed light emission by symbiotic *Vibrio fischeri* of the sepiolid squid *Euprymna scolopes*. Journal of Bacteriology 172: 3701–3706.

Bottomley MJ, Muraglia E, Bazzo R, and Carfi A. (2007). Molecular insights into quorum sensing in the human pathogen *Pseudomonas aeruginosa* from the structure of the virulence regulator LasR bound to its autoinducer. Journal of Biological Chemistry 282: 13592-13600.

Brosius J, Holy A. (1986). Regulation of ribosomal RNA promoters with a synthetic *lac* operator. Proceedings of the National Academy of Sciences 22: 6929-6933.

Castang S, Reverchon S, Gouet P, Nasser W. (2006). Direct evidence for the modulation of the activity of the *Erwinia chrysanthemi* quorum-sensing regulator ExpR by acylhomoserine lactone pheromone. Journal of Biological Chemistry 281: 29972-29987.

Chakrabarti S and Sowdhamini R. (2003). Functional sites and evolutionary connections of acylhomoserine lactone synthases. Protein Engineering Design & Selection 16: 271-278.

Chen X, Schauder S, Potier N, Van Dorsselaer A, Pelczer I, Bassler BL, and Hughson FM. (2002). Structural identification of a bacterial quorum-sensing signal containing boron. Nature 415: 545-459.

Choi SH, Greenberg EP. (1991). The C-terminal region of the *Vibrio fischeri* LuxR protein contains an inducer-independent *lux* gene activating domain. Proceedings of the National Academy of Sciences 24: 11115-11119.

Choi SH and Greenberg EP. (1992). Genetic dissection of DNA binding and luminescence gene activation by the *Vibrio fischeri* LuxR protein. Journal of Bacteriology 12: 4064-4069.

Cvitkovitch DG, Li YH, and Ellen RP. (2003). Quorum sensing and biofilm formation in Streptococcal infections. Journal of Clinical Investigation 112: 1626-1632.

Devine JH, Shadel GS, Baldwin TO. (1989). Identification of the operator of the *lux* regulon from the *Vibrio fischeri* strain ATCC7744. Processings of the National Academy of Sciences 86: 5688-5692.

De Keersmaecker SCJ, Sonck K, and Vanderleyden J. (2006). Let LuxS speak up in AI-2 signaling. Trends in Microbiology 14: 114-119.

Defoirdt T, Boon N, Sorgeloos P, Verstraete W, and Bossier P. (2008). Quorum sensing and quorum quenching in *Vibrio harveyi*: lessons learned from *in vivo* work. The ISME Journal 2: 19-26.

Dykxhoorn DM**,** St Pierre R**,** Linn T. (1996). A set of compatible *tac* promoter expression vectors. Gene 177: 133-136.

Eberhard A, Burlingame AL, Eberhard C, Kenyon GL, Nealson KH, and Oppenheimer NJ. (1981). Structural identification of autoinducer of *Photobacterium fischeri* luciferase. Biochemistry 20: 2444-2449.

Engebrecht J, Nealson K, and Silverman M. (1983). Bacterial bioluminescence: isolation and genetic analysis of functions from *Vibrio fischeri*. Cell 32: 773-781.

Engebrecht J and Silverman M. (1984). Identification of genes and gene products necessary for bacterial bioluminescence. Proceedings of the National Academy of Sciences USA 81: 4154-4158.

Engebrecht J and Silverman M. (1987). Nucleotide sequence of the regulatory locus controlling expression of bacterial genes for bioluminescence. Nucleic Acids Research 15: 10455-10467.

Finney AH, Blick RJ, Murakami K, Ishihama A, Stevens AM. (2002). Role of the C-terminal domain of the alpha subunit of RNA polymerase in LuxR-dependent transcriptional activation of the *lux* operon during quorum sensing. Journal of Bacteriology 184: 4520-4528.

Fuqua C, Parsek MR, and Greenberg EP. (2001). Regulation of gene expression by cell-to-cell communication: acyl-homoserine lactone quorum sensing. Annual Review of Genetics 35: 439-468.

Fuqua C and Greenberg EP. (2002). Listening in on bacteria: acyl-homoserine lactone signaling. Nature 3: 685-695.

Gonzalez JE and Keshavan ND. (2006). Messing with bacterial quorum sensing. Microbiology and Molecular Biology Reviews 70: 859-875.

Gould TA, Schweizer HP, and Churchill MEA. (2004). Structure of the *Pseudomonas aeruginosa* acyl-homoserinelactone synthase LasI. Molecular Microbiology 53: 1135-1146.

Grant SG, Jessee JB, Bllom FR, and Hanahan D. (1990). Differential plasmid rescue from transgenic mouse DNAs into *Escherichia coli* methylation-restriction mutants. Proceedings of the Nattional Academy of Sciences USA 87: 4645-4649.

Guzman LM, Belin D, Carson MJ, and Beckwith J. (1995). Tight regulation modulation and high level expression by vectors containing the arabinose P_{BAD} promoter. Journal of Bacteriology 177: 4121-4130.

Hanahan D. (1983). Studies on transformation of *Escherichia coli* with plasmids. Journal of Molecular Biology 166:557-580.

Johnson DC, Ishihama A, Stevens AM. (2003). Involvement of region 4 of the sigma 70 subunit of RNA polymerase in transcriptional activation of the *lux* operon during quorum sensing. FEMS Microbiology Letters 228: 193-201.

Joint I, Downie JA, and Williams P. (2007). Bacterial conversations: talking, listening, and eavesdropping. An introduction. Philosophical Transactions of the Royal Society of Britian 362: 1115-1117.

Kendall MK, Rasko DA, and Sperandio V. (2007). Global effects of the cell-to-cell signaling molecules autoinducer-2, autoinducer-3, and epinephrine in a *luxS* mutant of enterohemorrhagic *Escherichia coli*. Infection and Immunity 74: 4875-4884.

Kong KF, Vuong C, Otto M. (2006). *Staphylococcus* quorum sensing in biofilm formation and infection. International Journal of Medical Microbiology 296: 133-139.

Koutsoudis MD, Taltas D, Minogue TD, von Bodman SB. (2006). Quorum-sensing regulation governs bacterial adhesion, biofilm development, and host colonization in *Pantoea stewartii* subspecies *stewartii*. Proceedings of the National Academy of Sciences 103: 5983-5988.

Lee K-H, and Ruby E G. (1994). Effect of the squid host on the abundance and distribution of symbiotic *Vibrio fischeri* in nature. Applied Environmental Microbiology 60: 1565–1571.

Lyon GJ and Novick RP. (2004). Peptide signaling in *Staphylococcus aureus* and other Gram-positive bacteria. Peptides 25: 1389-1403.

McFall-Ngai M J. (1990). Crypsis in the pelagic environment. American Zoology 30: 175–188.

Meighen EA. (1991). Molecular biology of bacterial bioluminescence. Microbiology Reviews 55: 123-142.

Miller MB and Bassler BL. (2001). Quorum sensing in bacteria. Annual Reviews of Microbiology 55: 165-199.

Minogue TD, Wehland-von T, Bernhard F, and von Bodman SB. (2002). The autoregulatory role in EsaR, a quorum-sensing regulator in *Pantoea stewartii*: evidence for a repressor function. Molecular Microbiology 44: 1625-1635.

Moré MI, Finger LD, Stryker JL, Fuqua C, Eberhard A, Winans SC. (1996). Enzymatic synthesis of a quorum-sensing autoinducer through use of defined substrates. Science 272: 1655-1658.

Morohoshi T, Nakamura Y, Yamazaki G, Ishida A, Kato N, Ikeda T. (2007). The plant pathogen *Pantoea ananatis* produces N-acylhomoserine lactone and causes center rot disease of onion by quorum sensing. Journal of Bacteriology 189: 8333-8338.

Nasser W and Reverchon S. (2007). New insights into the regulatory mechanisms of the LuxR family of quorum sensing regulators. Analytical and Bioanalytical Chemistry 387: 381-390.

Nealson KH, Platt T, and Hastings JW. (1970). Cellular control of the synthesis and activity of the bacterial luminescent system. Journal of Bacteriology 104: 313-322.

Neiditch MB, Federle MJ, Miller ST, Bassler BL, Hughson FM. (2005). Regulation of LuxPQ receptor activity by the quorum-sensing signal autoinducer-2. Molecular Cell 18: 507-18.

Niesen FH, Berglund H, Vedadi M. (2007). The use of differential scanning fluorimetry to detect ligand interactions that promote protein stability. Nature Protocols 2: 2212-2221.

Nijvipakul S, Wongratana J, Suadee C, Entsch B, Ballou DP, Chaiyen P. (2008). LuxG is a functioning flavin reductase for bacterial luminescence. Journal of Bacteriology 190: 1531-1538.

Nimtz M, Mort A, Wray V, Domke T, Zhang Y, Coplin DL, Geider K. (1996). Structure of stewartan, the capsular exopolysaccharide from the corn pathogen *Erwinia stewartii*. Carbohydrate Research 288: 189-201.

Nouwens AS, Beatson SA, Whitchurch CB, Walsh BJ, Schweizer HP, Mattick JS, Cordwell SJ. (2003). Proteome analysis of extracellular proteins regulated by the *las* and *rhl* quorum sensing systems in *Pseudomonas aeruginosa* PAO1. Microbiology 149: 1311-1322.

Pappas KM, Weingart CL, and Winans SC. (2004). Chemical communication in proteobacteria: biochemical and structural studies of signal synthases and receptors required for intracellular signaling. Molecular Microbiology 53: 755-769.

Pataky JK. (2003). Stewart's wilt of corn. *In* M. L. Elliott (ed.), APSnet Feature Story. American Phytopathological Society, St. Paul. MN.

Ruby EG. (1996). Lessons from a cooperative, bacterial-animal association: the *Vibrio fischeri-Euprymna scolopes* light organ symbiosis. Annual Reviews of Microbiology 50: 591–624

Reading NC and Sperandio V. (2006). Quorum sensing: the many languages of bacteria. FEMS Microbiology Letters 254: 1-11.

Reverchon S, Bouillant ML, Salmond G, Nasser W. (1998). Integration of the quorum-sensing system in the regulatory networks controlling virulence factor synthesis in *Erwinia chrysanthemi*. Molecular Microbiology 6: 1407:1418.

Schaeffer AL, Val DL, Hanzelka BL, Cronan Jr JE, and Greenberg EP. (1996). Generation of cell-to-cell signals in quorum sensing: Acyl homoserine lactone synthase activity of a purified *Vibrio fischeri* LuxI protein. Proceedings of the National Academy of Sciences 93: 9505-9509.

Schuster M and Greenberg EP. (2006). A network of networks: quorum-sensing gene regulation in *Pseudomonas aeruginosa*. International Journal of Medical Microbiology 296: 73-81.

Shadel GS and Bladwin TO. (1992). Positive autoregulation of the *Vibrio fischeri luxR* gene. Journal of Biological Chemistry 267: 7696-7702.

Shafikhani S, Siegel RA, Ferrari E, and Schellenberger V. (1997). Generation of large libraries of random mutants in *Bacillus subtilis* by PCR-based plasmid multimerization. BioTechniques 23: 304-310.

Simon R, O'Connell M, Labes M, Puhler A. (1986). Plasmid vectors for the genetic analysis and manipulation of rhizobia and other Gram-negative bacteria. Methods in Enzymology 118:640–659.

Smith D, Wang JH, Swatton JE, Davenport P, Price B, Mikkelsen H, Stickland H, Nishikawa K, Gardiol N, Spring DR, and Welch M. (2006). Variations on a theme: diverse *N*-acyl homoserine lactone-mediated quorum sensing mechanisms in Gram-negative bacteria. Science Progress 89: 167-211.

Sperandio V, Mellies JL, Nguyen W, Shin S, an Kaper JB. (1999). Quorum sensing controls expression of the type III secretion gene transcription and protein secretion in enterohemorrhagic an enteropathogenic *Escherichia coli*. Proceedings of the National Academy of Sciences 96: 15196-15201.

Sperandio V, Torres AG, Jarvis, Nataro JP, and Kaper JB. (2003). Bacteria-host communication: the language of hormones. Proceedings of the National Academy of Sciences 100: 8951-8956.

Stevens AM and Greenberg EP. (1997). Quorum sensing in *Vibrio fischeri*: essential elements for activation of the luminescent genes. Journal of Bacteriology 179: 557-562.

Stevens AM and Greenberg EP. (1999). Transcriptional activation by LuxR, pp. 231-242. *In*: Cell-Cell Communication in Bacteria (G. M. Dunny and S. C. Winans, eds.), ASM Press Washington D.C.

Swartzman A, Kapoor S, Graham AF, and Meighen EA. (1990). A new *Vibrio fischeri lux* gene precedes a bidirectional termination site for the *lux* operon. Journal of Bacteriology 172: 6797-6802.

Swiderska A, Berndtson AK, Cha MR, Li L, Beaudoin GMJ, Zhu J, and Fuqua C. (2001). Inhibition of the *Agrobacterium tumefaciens* TraR quorum sensing regulator. Journal of Biological Chemistry 276: 49449-49458.

Taga ME and Bassler BL. (2003). Chemical communication among bacteria. Proceedings of the National Academy of Sciences USA 100: 14549-14554.

Urbanowski ML, Lostroh CP, Greenberg EP. (2004). Reversible acyl-homoserine lactone binding to purified *Vibrio fischeri* LuxR protein. Journal of Bacteriology 186: 631-637.

Vannini A, Volpari C, Gargiolo C, Muraglia E, Cortese R, De Francesco R, Neddermann P, and Di Marco S. (2002). The crystal structure of the quorum sensing protein TraR bound to its autoinducer and target DNA. The EMBO Journal 21: 4393-4401.

Vendeville A, Winzer K, Heurkier K, Tang CM, and Hardie KR. (2005). Making 'sense' of metabolism: autoinducer-2, LuxS and pathogenic bacteria. Nature 3: 383-396.

Visick KL and McFall-Ngai MJ. (2000). An exclusive contract: specificity in the *Vibrio fischeri-Euprymna scolopes* partnership. Journal of Bacteriology 7: 1779-1787.

Visick KL and Ruby EG. (2006). *Vibrio fischeri* and its host: it takes two to tango. Current Opinion in Microbiology 9: 632-638.

von Bodman SB, and Farrand SK. (1995). Capsular polysaccharide biosynthesis and pathogenecity in *Erwinia stewartii* require induction by an N-acylhomoserine lactone autoinducer. Journal of Bacteriology 177: 5000-5008.

von Bodman SB, Majerczak DR, and Coplin DL. (1998). A negative regulator mediates quorum-sensing control of exopolysaccharide production in *Pantoea stewartii* subsp. *Stewartii*. Proceedings of the National Academy of Sciences 95: 7687-7692.

von Bodman SB, Ball JK, Faini MA, Herrera CM, Minogue TD, Urbanowski ML, and Stevens AM. (2003). The quorum sensing negative regulators EsaR and $ExpR_{Ecc}$, homologues within the LuxR family, retain the ability to function as activators of transcription. Journal of Bacteriology 185: 7001-7007.

von Bodman SB, Carlier AL, and Stevens AM. (2008). The role of quorum sensing regulation in the pathogenesis of *Pantoea stewartii* subsp. *stewartii*. *In*: Chemical Communication Among Microbes (Winans, SW and Bassler, BL, eds). ASM Press Washington, D.C.

Walters M and Sperandio V. (2006). Autoinducer 3 and epinephrine signaling in the kinetics of locus of enterocyte effacement gene expression in enterohemorrhagic *Escherichia coli*. Infectious Immunity 74: 5445–5455.

Waters CM and Bassler BL. (2005). Quorum sensing: cell-to-cell communication in bacteria. Annual Review of Cell Developmental Biology 21: 319-346.

Watson WT, Minogue TD, Val DL, Beck von Bodman S, and Churchill MEA. (2002). Structural basis and specificity of acyl-homoserine lactone signal production in bacterial quorum sensing. Molecular Cell 9: 685-694.

White CE and Winans SC. (2007). Cell-cell communication in the plant pathogen *Agrobacterium tumefaciens*. Philosophical Transactions of The Royal Society B 362: 1471-297.

Whitehead NA, Barnard AML, Slater H, Simpson NJL, and Salmond GPC. (2001). Quorum sensing in Gram-negative bacteria. FEMS Microbiology Reviews 25: 365-404.

Wilson T and Hastings JW. (1998). Bioluminescence. Annual Review of Cell Developmental Biology 14: 197-230.

Zhang RG, Pappas T, Brace JL, Miller PC, Oulmassov T, Molyneaux JM, Anderson JC, Bashkin JK, Winans SC, and Joachimiak A. (2002). Structure of a bacterial quorum-sensing transcription factor complexed with pheromone and DNA. Nature 417: 971-974.